A Finite Difference Method for Solution of Integer-order and Caputo Fractional-time Advection-Diffusion-Reaction Equations: Convergence Analysis and Application to Air Pollution

Surattana Sungnul, Kanokwarun Para, Elvin J. Moore, Sekson Sirisubtawee and Sutthisak Phongthanapanich

***Abstract*—Proofs are given for the consistency, stability and convergence of the implicit forward-time central-space (FTCS) finite difference method for solving integer-order three-dimensional advection-diffusion-reaction equations (ADRE) and Caputo fractional-order two dimensional ADRE models. The method is then applied to obtain numerical solutions for the transport of pollutants in street tunnels with various reaction coefficients and rates of change of concentrations of sources and sinks of pollution. Examples are given for both integer-order and Caputo fractional-time systems.**

***Index Terms*—advection-diffusion-reaction equation, Caputo fractional derivative, finite difference method, convergence, pollutant concentration**

I. Introduction

For many years, integer-order advection-diffusion-reaction equations (ADRE) have been widely used as models in many areas of science and engineering, for example, in fluid flow, aerodynamics, fiber optics, water and air pollution, molecular diffusion and chemical engineering. Also, in recent years it has been recognized that if a physical system has memory or history effects then fractional derivatives can give better models. Because of their importance, there are many analytical and numerical methods that have been developed to solve both integer-order and fractional-order equations for both linear and nonlinear ADREs. However, in general, it is necessary to use numerical methods to solve most real-world problems.

A summary of some of the methods used for integer-order equations is as follows. In 2012, Garzón-Alvarado et al. [1] used a finite element method to solve a model of a decoupled system of ADREs based on Navier-Stokes equations. In 2012, Savovic and Djordjevich [2] developed an explicit finite difference method for solving a 1D advection-diffusion equation for three dispersion problems. In 2013, Appadu and Gidey [3] proposed two time-splitting procedures for solving a 2D advection-diffusion equation with constant coefficients. In 2013, Bause and Schwegler [4] developed a finite element method for solving systems of coupled convection-dominated transport equations. In 2015, Mojtabi and Deville [5] used separation of variables to obtain an analytical solution, and a finite element method to obtain a numerical solution, of a time-dependent 1D linear advection-diffusion equation. In 2016, Gharehbaghi [6] proposed explicit and implicit differential quadrature methods to compute numerical solutions of a time-dependent 1D advection-diffusion equation in a semi-infinite domain. In 2017, Gyrya and Lipnikov [7] developed a mimetic finite difference method on polygonal meshes for solution of diffusion equations with a tensorial diffusion coefficient. In 2017, Bahar and Gurarslan [8] studied Lie-Trotter and Strang splitting methods for solution of a 1D advection-diffusion equation. In 2018, Al-Jawary et al. [9] proposed a semi-analytical technique for finding exact solutions of Burgers' equations and applied the technique to study diffusion and advection-diffusion equations. In 2018, Lou et al. [10] proposed discontinuous Galerkin methods for solving linear advection-diffusion equations on unstructured hybrid grids. In 2018, Bhatt et al. [11] developed a Krylov subspace approximation-based locally extrapolated exponential time differencing method for solving nonlinear 3D ADRE systems. In 2020, Heng and Guodong [12] improved the element-free Galerkin method and used it for solving 3D advection-diffusion problems. In 2020, Cruz-Quintero and Jurado [13] proposed a backstepping design for boundary control of a reaction-advection-diffusion equation with constant coefficients. In 2021, Para et al. [14] developed a finite volume method for solving convection-diffusion problems on 2D triangular grids and compared the accuracy of the solutions with four piecewise linear reconstruction techniques, namely, least squares, Frink, Green-Gauss, and Holmes-Connell methods. In 2021, Hong et al. [15] used

Manuscript received March 12, 2024; revised September 6, 2024.

This research was funded by Faculty of Applied Science, King Mongkut's University of Technology North Bangkok, THAILAND (Contract no. 661132).

Surattana Sungnul is Associate Professor in the Department of Mathematics, King Mongkut's University of Technology North Bangkok, 10800 THAILAND and researcher in the Center of Excellence in Mathematics, 10400 THAILAND (corresponding author, e-mail: surattana.s@sci.kmutnb.ac.th).

Kanokwarun Para is Special Lecturer in the Department of Mathematics, King Mongkut's University of Technology North Bangkok, 10800 THAILAND (e-mail: kanokwarun.warun@gmail.com)

Elvin J. Moore is Foreign Lecturer in the Department of Mathematics, King Mongkut's University of Technology North Bangkok, 10800 THAILAND and researcher in the Center of Excellence in Mathematics, 10400 THAILAND (e-mail: elvin.j@sci.kmutnb.ac.th).

Sekson Sirisubtawee is Associate Professor in the Department of Mathematics, King Mongkut's University of Technology North Bangkok, 10800 THAILAND and researcher in the Center of Excellence in Mathematics, 10400 THAILAND (e-mail:sekson.s@sci.kmutnb.ac.th).

Sutthisak Phongthanapanich is Professor in the Department of Mechanical Engineering Technology, College of Industrial Technology, King Mongkut's University of Technology North Bangkok 10800 THAILAND (e-mail: sutthisak.p@cit.kmutnb.ac.th).

a meshless numerical scheme and a backward substitution method to solve 3D advection-diffusion equations. In 2021, Hidayat [16] proposed a meshless B-spline finite difference method for the numerical solution of ADRE problems. In 2021, Sun et al. [15] used a backward substitution method to solve 3D advection-diffusion equations. In 2021, Shahid et al. [17] studied an epidemic-type model with advection and diffusion terms for the transmission of computer viruses. In 2021, García and Jurado [18] designed an adaptive boundary control for a reaction-advection-diffusion PDE with unknown advection and reaction parameters.

In recent years, time or space fractional-order derivatives have been used to generalize many integer-order models of real-world problems in physics, applied mathematics, and engineering. The usual reason given for these generalizations is that the fractional-order equations give better models for real-life problems that include the memory effects or the past history of the system. There are now many definitions of fractional derivatives including Riemann-Liouville [19], Caputo [19], [20], Caputo-Fabrizio [21], Hadamard [22], Hilfer [23], [24], Katugampala [25], Atangana [26] and Hattaf [27], [28]. Some examples of recent research which are relevant to the numerical solution of fractional-order partial differential equations related to an ADRE are as follows. In 2005, Langlands and Henry [29] investigated the accuracy and stability of an implicit numerical scheme for solving a fractional diffusion equation describing anomalously diffusing particles. In 2009, Su et al. [30] employed a fractional Crank-Nicholson method (FCN) based on a shifted Grünwald-Letnikov formula, to solve a two-sided fractional advection-diffusion equation. In 2011, Wang [31] developed a fast characteristic finite difference method for efficient solution of space-fractional transient advection-diffusion equations in one space dimension. In 2018, Zhong et al. [32] used Legendre polynomials and the associated operational matrix to reduce fractional convection diffusion equations with time-space variable coefficients to corresponding algebraic systems which can be solved numerically. In 2018, Macías-Díaz [33] employed a finite difference method to solve fractional-order generalizations of the Burgers-Fisher and the Burgers-Huxley equations in multiple dimensions that included Riesz fractional diffusion. In 2018, Jannelli et al. [34] used Lie transformations to find analytical and numerical solutions of a time and space fractional ADRE. In 2019, Vivek et al. [35] studied the existence and stability of solutions to a partial differential equation using the Growall inequality method to prove Ulam-type stability. In 2021, El-Kahlout [36] used the integral Fourier-sine and integral Laplace transforms to obtain exact solutions of two types of partial differential equations of Caputo fractional order in the xz plane. In 2023, Qazza et al. [37] used a direct power series method to solve several types of Caputo time-fractional partial differential equations and systems. In 2023, Dimitrov et al. [38] considered an approximation of the Caputo fractional derivative and its asymptotic expansion formula and applied it to the time fractional Black–Scholes equation for option pricing. In 2024, Kumawat et al. [39] developed a new integral transform called the Khalouta transform and used it to find exact results of fractional differential equations using both Riemann-Liouville and Caputo fractional derivatives.

As stated above, one aim of the present paper is to use 2D and 3D ADRE models to study air pollution in street tunnels. Some recent papers relevant to pollution are as follows. In 2017, Oyjindal and Pochai [40] used explicit finite difference methods to obtain numerical simulations of air pollution near an industrial zone. In 2018, Suebyat and Pochai [41] used finite difference methods to solve a 3D air pollution model for a heavy traffic area under a Bangkok sky train platform. In 2018, Kusuma et al. [42] developed a finite difference method to solve 2D advection and 3D diffusion models of pollution distribution in a street tunnel. In 2020, Pananu et al. [43] analyzed the convergence of the implicit FTCS finite difference model for solving 2D ADRE and applied the scheme to pollutant dispersion in a reservoir. In 2022, Para et al. [44] proposed an explicit characteristic-based finite volume method for the numerical solution of 1D and 2D ADRE and applied it to solve some water pollution problems.

The main aims of the present paper are to develop implicit FTCS finite difference methods for numerical solution of integer-order 3D and fractional-order 2D ADRE models and to give proofs of stability and convergence of the methods. Then to apply the methods to obtain numerical solutions for some useful models of air pollution in street tunnels.

This paper is organized as follows. In section II, we introduce the integer-order 3D ADRE boundary value problem and then derive the integer-order implicit FTCS method and give analytical proofs of consistency, stability and convergence of the method. In section III, we introduce the Caputo fractional-order 2D ADRE boundary value problem and then derive the fractional-order implicit FTCS method and give analytical proofs of consistency and stability of the method. In section IV, we give numerical results for 2D and 3D ADRE models for air pollution in street tunnels using both the integer-order and fractional-order implicit FTCS methods. Finally, in section V we present conclusions.

II. Integer-Order Theory

We consider the following initial time, space boundary value problem for the 3D ADRE

$$\frac{\partial \Phi(\mathbf{x},t)}{\partial t} + \nabla \cdot \big(\mathbf{v}\Phi(\mathbf{x},t) - D(\mathbf{x})\nabla\Phi(\mathbf{x},t)\big) + R\Phi(\mathbf{x},t) = Q(\mathbf{x},t), \quad (1)$$

where $(\mathbf{x},t) \in \Omega \times [0,T]$, the initial time condition is

$$\Phi(\mathbf{x},0) = \psi(\mathbf{x}) \quad \text{for} \quad \mathbf{x} \in \Omega, \quad (2)$$

and the boundary space conditions are either Dirichlet or Neumann conditions given by

$$\begin{aligned} &\text{Dirichlet} && \Phi(\mathbf{x},t) = \psi_D(\mathbf{x},t), \\ &\text{Neumann} && D(\mathbf{x})\frac{\partial \Phi(\mathbf{x},t)}{\partial \mathbf{n}} = \psi_N(\mathbf{x},t) \\ & && \text{for} \quad (\mathbf{x},t) \in \partial\Omega \times [0,T]. \end{aligned} \quad (3)$$

In Eqs. (1)–(3), T is a finite time, $\partial\Omega$ is the boundary of the spatial domain Ω, the initial and boundary functions ψ, ψ_D and ψ_N are given functions, $\mathbf{v}$ is an advection vector, $D(\mathbf{x}) > 0$ is a diffusion coefficient function, R is a reaction constant, $Q(\mathbf{x},\mathbf{t})$ is a given source function, and $\mathbf{n}$ is a unit normal vector at the surface.

A. *Integer-order implicit FTCS method*

The first step in developing the finite difference method is to discretize Ω, $\partial\Omega$ and $[0,T]$. We assume that the spatial domain Ω is a rectangular solid of side lengths L_x, L_y and L_z in the x, y and z directions, respectively, and that there are N_x step sizes of length Δx in the x direction, N_y step sizes of length Δy in the y direction and N_z step sizes of length Δz in the z direction. Then $L_x = N_x\Delta x$, $L_y = N_y\Delta y$ and $L_z = N_z\Delta z$ and the discretized version of Ω is the spatial grid

$$\begin{aligned}\Omega_h &= \{(x_i,y_j,z_k)\,|\,x_i = i\Delta x,\ y_j = j\Delta y,\ z_k = k\Delta z,\\ &\quad i = 0,1,\ldots,N_x,\ j = 0,1,\ldots,N_y,\\ &\quad k = 0,1,\ldots,N_z\},\end{aligned} \tag{4}$$

and the boundary of the spatial grid is

$$\begin{aligned}\partial\Omega_h &= \{x_0 = 0;\ y_j = j\Delta y,\ j = 0,1,\ldots,N_y;\\ &\quad z_k = k\Delta z,\ k = 0,1,\ldots,N_z\}\\ &\cup\{x_{N_x} = L_x;\ y_j = j\Delta y,\ j = 0,1,\ldots,N_y;\\ &\quad z_k = k\Delta z,\ k = 0,1,\ldots,N_z\}\\ &\cup\{x_i = i\Delta x,\ i = 0,1,\ldots,N_x;\ y_0 = 0;\\ &\quad z_k = k\Delta z,\ k = 0,1,\ldots,N_z\}\\ &\cup\{x_i = i\Delta x,\ i = 0,1,\ldots,N_x;\ y_{N_y} = L_y;\\ &\quad z_k = k\Delta z,\ k = 0,1,\ldots,N_z\}\\ &\cup\{x_i = i\Delta x,\ i = 0,1,\ldots,N_x;\\ &\quad y_j = j\Delta y,\ j = 0,1,\ldots,N_y;\ z_0 = 0\}\\ &\cup\{x_i = i\Delta x,\ i = 0,1,\ldots,N_x;\\ &\quad y_j = j\Delta y,\ j = 0,1,\ldots,N_y;\ z_{N_z} = L_z\}.\end{aligned} \tag{5}$$

For the time interval $[0,T]$, we will assume that there are N steps of size $\Delta t = \frac{T}{N}$ and then

$$T_N = \{t^n \mid t^n = n\Delta t,\quad n = 0,1,\ldots,N\}. \tag{6}$$

In the proofs of convergence of the implicit FTCS method, we will assume that the velocity and diffusion functions are constant. The component form of the initial-boundary value problem in Eqs. (1)–(3) is then as follows:

$$\begin{aligned}&\frac{\partial\Phi}{\partial t} + u\frac{\partial\Phi}{\partial x} + v\frac{\partial\Phi}{\partial y} + w\frac{\partial\Phi}{\partial z}\\ &\quad -D_x\frac{\partial^2\Phi}{\partial x^2} - D_y\frac{\partial^2\Phi}{\partial y^2} - D_z\frac{\partial^2\Phi}{\partial z^2} + R\Phi = Q(x,y,z,t),\\ &\text{where } \Phi = \Phi(x,y,z,t),\\ &\quad (x,y,z)\in[0,L_x]\times[0,L_y]\times[0,L_z],\ t\in[0,T]\\ &\text{and where}\quad \Phi(x,y,z,0) = \psi(x,y,z),\\ &\quad \Phi(0,y,z,t) = \alpha_1(y,z,t),\ \Phi(L_x,y,z,t) = \alpha_2(y,z,t),\\ &\quad \Phi(x,0,z,t) = \beta_1(x,z,t),\ \Phi(x,L_y,z,t) = \beta_2(x,z,t),\\ &\quad \Phi(x,y,0,t) = \eta_1(x,y,t),\ \Phi(x,y,L_z,t) = \eta_2(x,y,t).\end{aligned} \tag{7,8}$$

Here, (u,v,w) are constant velocities in the (x,y,z) directions, (D_x,D_y,D_z) are constant diffusion coefficients in the (x,y,z) directions, and we have assumed that the initial function $\psi(x,y,z)$ is a given function and that the space conditions are Dirichlet conditions with given functions $\alpha_1(y,z,t)$, $\alpha_2(y,z,t)$, $\beta_1(x,z,t)$, $\beta_2(x,z,t)$, $\eta_1(x,y,t)$ and $\eta_2(x,y,t)$.

As the next step, we discretize the domain as $(x_i,y_j,z_k,t_n)\in\Omega_h\times T_N$, where the spatial grid Ω_h and boundary grid $\partial\Omega_h$ are defined in Eqs. (4) and (5), respectively, and the time grid $T_N = [0,T]$ is defined in (6).

In the remainder of the paper, we will use the following notation.

$$\Phi^n_{i,j,k} = \Phi(x_i,y_j,z_k,t^n). \tag{9}$$

In the implicit FTCS method, the finite difference approximations for the time and space derivatives and the truncation errors are as follows:

$$\begin{aligned}\frac{\partial\Phi(x_i,y_j,x_k,t^n)}{\partial t} &= \frac{\Phi^{n+1}_{i,j,k} - \Phi^n_{i,j,k}}{\Delta t} + O(\Delta t),\\ \frac{\partial\Phi(x_i,y_j,z_k,t^n)}{\partial x} &= \frac{\Phi^{n+1}_{i+1,j,k} - \Phi^{n+1}_{i-1,j,k}}{2\Delta x} + O((\Delta x)^2),\\ \frac{\partial^2\Phi(x_i,y_j,z_k,t^n)}{\partial x^2} &= \frac{\Phi^{n+1}_{i+1,j,k} - 2\Phi^{n+1}_{i,j,k} + \Phi^{n+1}_{i-1,j,k}}{(\Delta x)^2}\\ &\quad + O((\Delta x)^2),\end{aligned} \tag{10}$$

with similar approximations for y and z derivatives. As the implicit forward-time, central-space name implies, forward-time and central-space approximations are used for the derivatives and the space derivatives are approximated at time t^{n+1} in the step from time t^n to time t^{n+1}.

After substituting the finite difference approximations in Eq. (10) into the component equation (7)–(8), we obtain the following implicit FTCS approximation.

$$\begin{aligned}&\frac{\Phi^{n+1}_{i,j,k} - \Phi^n_{i,j,k}}{\Delta t} + u\frac{\Phi^{n+1}_{i+1,j,k} - \Phi^{n+1}_{i-1,j,k}}{2\Delta x} + v\frac{\Phi^{n+1}_{i,j+1,k} - \Phi^{n+1}_{i,j-1,k}}{2\Delta y}\\ &\quad + w\frac{\Phi^{n+1}_{i,j,k+1} - \Phi^{n+1}_{i,j,k-1}}{2\Delta z} - D_x\frac{\Phi^{n+1}_{i+1,j,k} - 2\Phi^{n+1}_{i,j,k} + \Phi^{n+1}_{i-1,j,k}}{(\Delta x)^2}\\ &\quad - D_y\frac{\Phi^{n+1}_{i,j+1,k} - 2\Phi^{n+1}_{i,j,k} + \Phi^{n+1}_{i,j-1,k}}{(\Delta y)^2}\\ &\quad - D_z\frac{\Phi^{n+1}_{i,j,k+1} - 2\Phi^{n+1}_{i,j,k} + \Phi^{n+1}_{i,j,k-1}}{(\Delta z)^2} + R\Phi^{n+1}_{i,j,k} = Q^n_{i,j,k},\end{aligned} \tag{11}$$

$$\begin{aligned}\text{subject to}\quad &\Phi^0_{i,j,k} = \xi_{i,j,k},\quad \Phi^n_{0,j,k} = \alpha^n_{1,j,k},\quad \Phi^n_{N_x,j,k} = \alpha^n_{2,j,k},\\ &\Phi^n_{i,0,k} = \beta^n_{1,i,k},\quad \Phi^n_{i,N_y,k} = \beta^n_{2,i,k},\quad \Phi^n_{i,j,0} = \eta^n_{1,i,j},\\ &\Phi^n_{i,j,N_z} = \eta^n_{2,i,j},\end{aligned} \tag{12}$$

where the truncation errors (T,E.) for (11) are

$$T.E. = O\left((\Delta t),(\Delta x)^2,(\Delta y)^2,(\Delta z)^2\right). \tag{13}$$

B. *Integer-order convergence analysis*

An initial time, space boundary value problem is called a well-posed problem if it has a unique solution. In this paper, we will assume that all ADRE problems are well-posed problems. A fundamental theorem that we use in the proof of consistency, stability and convergence of the implicit FTCS method is the following Lax equivalence theorem.

Theorem 2.1: (Lax equivalence theorem [45], [46]) A consistent finite difference method for a well-posed linear initial value problem is convergent if and only if it is also a stable method.

As the first step, we will prove that the implicit FTCS method is a consistent method for solving the ADRE.

Definition 2.1: Consistent method [45]–[47]

A finite difference method is a consistent method for a partial differential equation if the finite difference method converges

to the differential equation as the discrete mesh converges to the continuous domain.

Theorem 2.2: The implicit FTCS finite difference method in Eq. (11) is a consistent method for the ADRE in Eq. (7).

Proof: The truncation error in Eq. (13) between the FTCS method in Eq. (11) and the component form of the ADRE in Eq. (7) clearly converges to zero as $\Delta t \to 0$, $\Delta x \to 0$, $\Delta y \to 0$, $\Delta z \to 0$. The FTCS method is therefore a consistent method for the ADRE. ■

We now prove that the FTCS method is a stable method.

Definition 2.2: Stable [46], [47]

Basically, a finite difference scheme is said to be stable if the errors made at one iteration of the calculation do not cause the errors to be magnified as the computations are continued. In the remainder of this section, for ease of writing and without loss of generality, we will set $\Delta x = \Delta y = \Delta z = h$ and let $\tau = \Delta t$ and assume that $D_x = D_y = D_z = D$. We begin by looking at the homogeneous equation with the source term $Q^n_{i,j,k} = 0$. For a homogeneous linear difference equation, we can use the von Neumann method to prove the stability of the method [46], [47].

Case I: Homogeneous equation

Proof: Setting $Q^n_{i,j,k} = 0$ in equation (11), we obtain the discretized homogeneous version of (11). We can also note that the initial conditions in (12) uniquely specify the solution of (11) at initial time $n = 0$. Then, following the von Neumann method [47], we can assume that the solution for the homogeneous linear difference equation (11) is a linear combination of solutions of the form

$$\Phi^n_{i,j,k} = \lambda^n e^{I(\alpha i+\beta j+\eta k)}, \quad I = \sqrt{-1}, \tag{14}$$

where λ is an eigenvalue of the linear difference operator. Substituting the solution (14) into (11), we obtain the equation for an eigenvalue λ which can be rearranged into the simpler form

$$\begin{aligned}&\lambda^n e^{I(\alpha i+\beta j+\eta k)}\left[\frac{\lambda-1}{\tau}\right] + \lambda^{n+1} e^{I(\alpha i+\beta j+\eta k)} \times \\ &\Big[u\frac{e^{I\alpha}-e^{-I\alpha}}{2h} + v\frac{e^{I\beta}-e^{-I\beta}}{2h} + w\frac{e^{I\eta}-e^{-I\eta}}{2h} \\ &-D\big(\frac{e^{I\alpha}-2+e^{-I\alpha}}{h^2} + \frac{e^{I\beta}-2+e^{-I\beta}}{h^2} + \frac{e^{I\eta}-2+e^{-I\eta}}{h^2}\big) \\ &+R\Big] = 0.\end{aligned} \tag{15}$$

Then the only nonzero solution of (15) is

$$\lambda = \frac{1}{1+\frac{\tau}{h}\left[\frac{4D}{h}(A+IB+Rh)\right]}, \tag{16}$$

where $A = \sin^2\frac{\alpha}{2} + \sin^2\frac{\beta}{2} + \sin^2\frac{\eta}{2}$ and $B = u\sin\alpha + v\sin\beta + w\sin\eta$. Letting $\gamma = \frac{4D\tau}{h^2}$ and $\mu = \frac{\tau}{h}$, we find that the magnitude of λ is

$$\begin{aligned}|\lambda| &= \frac{1}{\sqrt{\left[1+\gamma A+R\tau\right]^2 + \left[\mu B\right]^2}}, \\ &\leq 1.\end{aligned} \tag{17}$$

Therefore, the condition for Von Neumann stability of a homogeneous linear difference equation that the magnitude of all eigenvalues are less than or equal to 1 has been proved for arbitrary values of time steps τ and space steps h. ■

Case II: Nonhomogeneous equation

We now prove the stability of the nonhomogeneous equation (11). A necessary condition for stability is that the initial condition function, the boundary functions and the source term in (11) are bounded, and therefore we will assume that

$$\begin{aligned}&|\psi_{i,j,k}| \leq \overline{\psi},\ |\alpha^n_{1,j,k}| \leq \overline{\alpha}_1,\ |\alpha^n_{2,j,k}| \leq \overline{\alpha}_2,\ |\beta^n_{1,i,k}| \leq \overline{\beta}_1, \\ &|\beta^n_{2,i,k}| \leq \overline{\beta}_2,\ |\eta^n_{1,i,j}| \leq \overline{\eta}_1,\ |\eta^n_{2,i,j}| \leq \overline{\eta}_2,\ |Q^n_{i,j,k}| \leq \overline{Q}\end{aligned} \tag{18}$$

for all values of (i, j, k, n) for some finite non-negative constants

$$\overline{\psi},\ \overline{\alpha}_1,\ \overline{\alpha}_2,\ \overline{\beta}_1,\ \overline{\beta}_2,\ \overline{\eta}_1,\ \overline{\eta}_2,\ \overline{Q}. \tag{19}$$

For simplicity, we will also define a maximum bound on all boundary conditions as

$$\overline{\omega} = \max\{\overline{\alpha}_1,\ \overline{\alpha}_2,\ \overline{\beta}_1,\ \overline{\beta}_2,\ \overline{\eta}_1,\ \overline{\eta}_2\}. \tag{20}$$

As the first step in the proof, we obtain bounds on the norms of $|\Phi^{n+1}_{i,j,k}|$ in the iteration from time step n to time step $n+1$. After rearranging the FTCS iteration equation (11) and setting $\Delta x = \Delta y = \Delta z = h$, $\Delta t = \tau$ and $D_x = D_y = D_z = D$, we can rewrite the iteration equation in the form

$$\begin{aligned}&a\Phi^{n+1}_{i-1,j,k} + b\Phi^{n+1}_{i,j-1,k} + c\Phi^{n+1}_{i,j,k-1} + d\Phi^{n+1}_{i,j,k} + e\Phi^{n+1}_{i+1,j,k} \\ &+f\Phi^{n+1}_{i,j+1,k} + g\Phi^{n+1}_{i,j,k+1} = -\Phi^n_{i,j,k} - \tau Q^n_{i,j,k},\end{aligned} \tag{21}$$

where

$$\begin{aligned}&a = \left(\frac{u\tau}{2h} + \frac{D\tau}{h^2}\right),\ b = \left(\frac{v\tau}{2h} + \frac{D\tau}{h^2}\right),\ c = \left(\frac{w\tau}{2h} + \frac{D\tau}{h^2}\right), \\ &d = \left(-1 - \frac{6D\tau}{h^2} - R\tau\right),\ e = \left(-\frac{u\tau}{2h} + \frac{D\tau}{h^2}\right), \\ &f = \left(-\frac{v\tau}{2h} + \frac{D\tau}{h^2}\right),\ g = \left(-\frac{w\tau}{2h} + \frac{D\tau}{h^2}\right),\end{aligned} \tag{22}$$

and where the step sizes τ and h can be chosen so that the coefficients a, b, c, d, e, f, g satisfy the conditions

$$|d| > |a| + |b| + |c| + |e| + |f| + |g| + \delta, \quad \delta > 0. \tag{23}$$

We now prove the following theorem.

Theorem 2.3: If the coefficients of Eq. (21) satisfy the conditions Eq. (23) then, for some value of δ, the solutions of Eq. (21) exist and satisfy the inequality

$$|\Phi^{n+1}_{i,j,k}| \leq \max\left\{\overline{\omega}, \frac{1}{\delta}\max_{i,j,k}|\Phi^n_{i,j,k}| + \frac{\tau\overline{Q}}{\delta}\right\}. \tag{24}$$

Proof: : Assume that

$$\begin{aligned}|\Phi^{n+1}_{i^*,j^*,k^*}| = \max_{i,j,k}\{|\Phi^{n+1}_{i,j,k}|\},\ i = 0,1,...,N_x, \\ j = 0,1,...,N_y,\ k = 0,1,...,N_z.\end{aligned} \tag{25}$$

Note: Eq. (25) implies that

$$\begin{aligned}|\Phi^{n+1}_{i^*,j^*,k^*}| \geq \max\Big\{&|\Phi^{n+1}_{i^*-1,j^*,k^*}|, |\Phi^{n+1}_{i^*+1,j^*,k^*}|, \\ &\Big|\Phi^{n+1}_{i^*,j^*-1,k^*}|, |\Phi^{n+1}_{i^*,j^*+1,k^*}|, \\ &|\Phi^{n+1}_{i^*,j^*,k^*-1}|, |\Phi^{n+1}_{i^*,j^*,k^*+1}|\Big\},\end{aligned} \tag{26}$$

and that from the upper bound conditions (18)–(20), we have:

$$|\Phi^{n+1}_{i,j,k}| \leq \max\left\{\overline{\omega}, |\Phi^{n+1}_{i^*,j^*,k^*}|\right\} \tag{27}$$

for all i, j, k. Then, from (21), we have

$$\begin{aligned}
&|d||\Phi^{n+1}_{i^*,j^*,k^*}| \\
&\quad = \quad |-a\Phi^{n+1}_{i^*-1,j^*,k^*} - b\Phi^{n+1}_{i^*,j^*-1,k^*} - c\Phi^{n+1}_{i^*,j^*,k^*-1} \\
&\qquad -e\Phi^{n+1}_{i^*+1,j^*,k^*} - f\Phi^{n+1}_{i^*,j^*+1,k^*} - g\Phi^{n+1}_{i^*,j^*,k^*+1} \\
&\qquad +\Phi^{n}_{i^*,j^*,k^*} + \tau Q^{n}_{i^*,j^*,k^*}| \\
&\quad \leq \quad |a\Phi^{n+1}_{i^*-1,j^*,k^*}| + |b\Phi^{n+1}_{i^*,j^*-1,k^*}| + |c\Phi^{n+1}_{i^*,j^*,k^*-1}| \\
&\qquad +|e\Phi^{n+1}_{i^*+1,j^*,k^*}| + |f\Phi^{n+1}_{i^*,j^*+1,k^*}| + |g\Phi^{n+1}_{i^*,j^*,k^*+1}| \\
&\qquad +|\Phi^{n}_{i^*,j^*,k^*}| + |\tau Q^{n}_{i^*,j^*,k^*}| \\
&\quad = \quad |a||\Phi^{n+1}_{i^*-1,j^*,k^*}| + |b||\Phi^{n+1}_{i^*,j^*-1,k^*}| + |c||\Phi^{n+1}_{i^*,j^*,k^*-1}| \\
&\qquad +|e||\Phi^{n+1}_{i^*+1,j^*,k^*}| + |f||\Phi^{n+1}_{i^*,j^*+1,k^*}| \\
&\qquad +|g||\Phi^{n+1}_{i^*,j^*,k^*+1}| + |\Phi^{n}_{i^*,j^*,k^*}| + \tau|Q^{n}_{i^*,j^*,k^*}| \\
&\quad \leq \quad (|a|+|b|+|c|+|e|+|f|+|g|)|\Phi^{n+1}_{i^*,j^*,k^*}| \\
&\qquad +|\Phi^{n}_{i^*,j^*,k^*}| + \tau\overline{Q}, \qquad (28)
\end{aligned}$$

and therefore

$$\begin{aligned}
|\Phi^{n+1}_{i^*,j^*,k^*}| \quad &\leq \quad \frac{|\Phi^{n}_{i^*,j^*,k^*}| + \tau\overline{Q}}{|d|-|a|-|b|-|c|-|e|-|f|-|g|} \\
&\leq \quad \frac{|\Phi^{n}_{i^*,j^*,k^*}|}{\delta} + \frac{\tau\overline{Q}}{\delta}. \qquad (29)
\end{aligned}$$

Then, from (18)–(20), and since

$$|\Phi^{n}_{i^*,j^*,k^*}| \leq \max_{i,j,k}|\Phi^{n}_{i,j,k}| \quad \text{and} \quad |\Phi^{n+1}_{i^*,j^*,k^*}| = \max_{i,j,k}|\Phi^{n+1}_{i,j,k}|, \qquad (30)$$

we have

$$|\Phi^{n+1}_{i,j,k}| \leq |\Phi^{n+1}_{i^*,j^*,k^*}| \leq \max\left\{\overline{\omega}, \frac{1}{\delta}\max_{i,j,k}|\Phi^{n}_{i,j,k}| + \frac{\tau\overline{Q}}{\delta}\right\} \qquad (31)$$

for all i, j, k. The proof is complete. ■

Note: Theorem 2.3 proves that if the maximum norm of the solution at the previous time step n exists, then the maximum norm of the solution at time step $n+1$ also exists and is a bounded multiple of the maximum norm of the solution at the previous time step.

By iteration of the result in Eq. (24) and using the initial condition bound on the initial condition in (18) that $|\Phi^{0}_{i,j,k}| = |\psi_{i,j,k}| \leq \overline{\psi}$, we have that

$$\begin{aligned}
|\Phi^{1}_{i,j,k}| \quad &\leq \quad \max_{i,j,k}|\Phi^{1}_{i,j,k}| \leq \max\left\{\overline{\omega}, \frac{1}{\delta}\overline{\xi} + \frac{\tau\overline{Q}}{\delta}\right\}, \\
|\Phi^{2}_{i,j,k}| \quad &\leq \quad \max_{i,j,k}|\Phi^{2}_{i,j,k}| \leq \max\left\{\overline{\omega}, \frac{1}{\delta}\max_{i,j,k}|\Phi^{1}_{i,j,k}| + \frac{\tau\overline{Q}}{\delta}\right\}, \\
&\vdots \\
|\Phi^{N}_{i,j,k}| \quad &\leq \quad \max_{i,j,k}|\Phi^{N-1}_{i,j,k}| \leq \max\left\{\overline{\omega}, \frac{1}{\delta}\max_{i,j,k}|\Phi^{N-1}_{i,j,k}| + \frac{\tau\overline{Q}}{\delta}\right\}, \qquad (32)
\end{aligned}$$

where N is the total number of steps. It is clear from the iteration in (32) that increasing the value of δ in Eq. (23), i.e., increasing the coefficient $|d|$ relative to the coefficients $|a|$, $|b|$,$|c|$,$|e|$,$|f|$,$|g|$, increases the accuracy and stability of the method.

Finally, we note that we have proved that the implicit FTCS finite difference method is consistent and stable and therefore by the Lax Equivalence Theorem, the method is also convergent.

III. Caputo Fractional-Time Theory

For simplicity, we consider the following Caputo fractional-time 2-dimensional version of the integer-order ADRE in Eqs. (1)–(3). We also assume that the advection velocity is a constant u in the x-direction.

$$\begin{aligned}
&\frac{\partial^\alpha \phi(\mathbf{x},t)}{\partial t^\alpha} + u\frac{\partial \phi(\mathbf{x},t)}{\partial x} - D\left(\frac{\partial^2 \phi(\mathbf{x},t)}{\partial x^2} + \frac{\partial^2 \phi(\mathbf{x},t)}{\partial y^2}\right) \\
&\qquad +R\phi(\mathbf{x},t) = Q(\mathbf{x},t), \\
&\mathbf{x} = (x,y) \in \Omega = (0,L_1)\times(0,L_2),\ t \in (0,T], \qquad (33)
\end{aligned}$$

with initial and boundary conditions:

$$\begin{aligned}
\phi(x,y,0) \quad &= \quad \psi(x,y),\ (x,y) \in \Omega, \qquad (34) \\
\phi(x,y,t)|_{\partial\Omega} \quad &= \quad 0,\ 0 \leq t \leq T, \qquad (35)
\end{aligned}$$

and where the Caputo fractional-time derivative of order $0 < \alpha < 1$ is defined by

$$\frac{\partial^\alpha \phi(x,y,t)}{\partial t^\alpha} = \frac{1}{\Gamma(1-\alpha)}\int_0^t \frac{\partial \phi(x,y,\xi)}{\partial \xi}\frac{d\xi}{(t-\xi)^\alpha}. \qquad (36)$$

A. *Fractional-order implicit FTCS method*

The following derivation is a generalization of the method discussed in Zhuang and Liu [48] for a Caputo fractional diffusion equation.

In the fractional differential equation (33), we discretize the Caputo fractional-time derivative in (36) using the discretization given in section (II-A) as follows:

$$\begin{aligned}
&\frac{\partial^\alpha \phi(x_i,y_j,t^{n+1})}{\partial t^\alpha} \\
&\quad = \frac{1}{\Gamma(1-\alpha)}\sum_{s=0}^{n}\int_{t^s}^{t^{s+1}} \frac{\partial \phi(x_i,y_j,\xi)}{\partial \xi}\frac{d\xi}{(t^{n+1}-\xi)^\alpha}, \qquad (37)
\end{aligned}$$

where $t^s = s\tau,\ s = 0,1,2,\ldots,N$. We then approximate the partial derivative in Eq. (37) by the finite difference approximation

$$\frac{\partial \phi(x_i,y_j,\xi)}{\partial \xi} = \frac{\phi(x_i,y_j,t^{s+1}) - \phi(x_i,y_j,t^s)}{\tau} + O(\tau) \qquad (38)$$

and obtain

$$\begin{aligned}
&\int_{t^s}^{t^{s+1}} \frac{\partial \phi(x_i,y_j,\xi)}{\partial \xi}\frac{d\xi}{(t^{n+1}-\xi)^\alpha} \\
&\quad = \frac{\phi(x_i,y_j,t^{s+1}) - \phi(x_i,y_j,t^s)}{\tau}\int_{t^s}^{t^{s+1}} \frac{d\xi}{(t^{n+1}-\xi)^\alpha} \\
&\quad = \frac{\tau^{-\alpha}\big(\phi(x_i,y_j,t^{s+1}) - \phi(x_i,y_j,t^s)\big)}{(1-\alpha)}b_{n-s} + O(\tau), \qquad (39)
\end{aligned}$$

where $b_{n-s} = (n-s+1)^{1-\alpha} - (n-s)^{1-\alpha}$. Therefore,

$$\begin{aligned}
&\frac{\partial^\alpha \phi(x_i,y_j,t^{n+1})}{\partial t^\alpha} \\
&= \frac{\tau^{-\alpha}}{(1-\alpha)\Gamma(1-\alpha)}\sum_{s=0}^{n}\big(\phi(x_i,y_j,t^{s+1}) - \phi(x_i,y_j,t^s)\big)b_{n-s} \\
&\qquad +O(\tau). \qquad (40)
\end{aligned}$$

Next, replacing $(1-\alpha)\Gamma(1-\alpha) = \Gamma(2-\alpha)$ and substituting $s = n-s$ and $b_s = (s+1)^{1-\alpha} - s^{1-\alpha}$ in

the sum, we have

$$\begin{aligned}&\frac{\partial^\alpha \phi(x_i,y_j,t^{n+1})}{\partial t^\alpha}\\&=\frac{\tau^{-\alpha}}{\Gamma(2-\alpha)}\sum_{s=0}^{n} b_s\big(\phi(x_i,y_j,t^{n-s+1})-\phi(x_i,y_j,t^{n-s})\big)\\&\qquad\qquad +O(\tau)\\&=L^\alpha_{h,\tau}\phi(x_i,y_j,t^{n+1})+O(\tau).\end{aligned}\tag{41}$$

Therefore, using (41), we have that the truncation error in the Caputo fractional derivative is

$$\left|\frac{\partial^\alpha \phi(x_i,y_j,t^{n+1})}{\partial t^\alpha}-L^\alpha_{h,\tau}\phi(x_i,y_j,t^{n+1})\right|\le C\tau,\tag{42}$$

where C is a constant greater than or equal to the sum of the absolute values of the errors in all terms.

Then, substituting the fractional time approximation Eq. (41) and the centered space finite differences in Eq. (10) into Eq. (33), we obtain, after rearranging, the following implict FTCS approximation for (33):

$$\begin{aligned}&\phi^{n+1}_{i,j}-\phi^n_{i,j}+\sum_{s=1}^{n} b_s\left(\phi^{n-s+1}_{i,j}-\phi^{n-s}_{i,j}\right)\\&\qquad +\tau^\alpha\Gamma(2-\alpha)u\left(\frac{\phi^{n+1}_{i+1,j}-\phi^{n+1}_{i-1,j}}{2\Delta x}\right)\\&=\tau^\alpha\Gamma(2-\alpha)D\left(\frac{\phi^{n+1}_{i+1,j}-2\phi^{n+1}_{i,j}+\phi^{n+1}_{i-1,j}}{(\Delta x)^2}\right.\\&\qquad\left.+\frac{\phi^{n+1}_{i,j+1}-2\phi^{n+1}_{i,j}+\phi^{n+1}_{i,j-1}}{(\Delta y)^2}\right)\\&\quad -\tau^\alpha\Gamma(2-\alpha)R\phi^{n+1}_{i,j}+\tau^\alpha\Gamma(2-\alpha)Q^{n+1}_{i,j},\end{aligned}\tag{43}$$

where $\phi^n_{i,j}=\phi(x_i,y_j,t^n)$ and $i=1,2,\ldots,N_1-1;\ j=1,2,\ldots,N_2-1;\ n=1,2,\ldots,N-1$.

Finally, letting

$$P_1=\frac{u\tau^\alpha\Gamma(2-\alpha)}{2\Delta x},\ P_2=\frac{D\tau^\alpha\Gamma(2-\alpha)}{(\Delta x)^2},\ P_3=\frac{D\tau^\alpha\Gamma(2-\alpha)}{(\Delta y)^2},\tag{44}$$

we obtain the following implicit fractional-time difference equation approximation (FDM) for (33).

$$\begin{aligned}&(P_1-P_2)\phi^{n+1}_{i+1,j}-(P_1+P_2)\phi^{n+1}_{i-1,j}\\&\quad+[1+2P_2+2P_3+\tau^\alpha\Gamma(2-\alpha)R]\phi^{n+1}_{i,j}\\&\quad-P_3(\phi^{n+1}_{i,j+1}+\phi^{n+1}_{i,j-1})\\&=\phi^n_{i,j}-\sum_{s=1}^{n} b_s\left(\phi^{n+1-s}_{i,j}-\phi^{n-s}_{i,j}\right)+\tau^\alpha\Gamma(2-\alpha)Q^{n+1}_{i,j}.\end{aligned}\tag{45}$$

From the definition of $b_s=(s+1)^{1-\alpha}-s^{1-\alpha}$, we have the following result.

Lemma 3.1: The coefficients $b_s(s=0,1,2,\ldots)$ satisfy:

$$\begin{aligned}&(1)\ b_0=1,\ b_s>0,\ s=0,1,2,\ldots;\\&(2)\ b_s>b_{s+1},\ s=0,1,2,\ldots.\end{aligned}$$

Hence, for $n=0$:

$$\begin{aligned}&(P_1-P_2)\phi^1_{i+1,j}-(P_1+P_2)\phi^1_{i-1,j}\\&\quad+[1+2P_2+2P_3+\tau^\alpha\Gamma(2-\alpha)R]\phi^1_{i,j}\\&\quad-P_3(\phi^1_{i,j+1}+\phi^1_{i,j-1})\\&=\psi(x_i,y_j)+\tau^\alpha\Gamma(2-\alpha)Q^1_{i,j},\end{aligned}\tag{46}$$

and for $n\ge 1$:

$$\begin{aligned}&(P_1-P_2)\phi^{n+1}_{i+1,j}-(P_1+P_2)\phi^{n+1}_{i-1,j}\\&\quad+[1+2P_2+2P_3+\tau^\alpha\Gamma(2-\alpha)R]\phi^{n+1}_{i,j}\\&\quad-P_3(\phi^{n+1}_{i,j+1}+\phi^{n+1}_{i,j-1})\\&=(b_0-b_1)\phi^n_{i,j}+\sum_{s=1}^{n-1}(b_s-b_{s+1})\phi^{n-s}_{i,j}+b_n\phi^0_{i,j}\\&\quad+\tau^\alpha\Gamma(2-\alpha)Q^{n+1}_{i,j},\end{aligned}\tag{47}$$

where $i=1,2,\ldots,N_1;\ j=1,2,\ldots,N_2$.

B. Fractional-order convergence analysis

As stated in the Lax theorem in subsection II-B, a consistent finite difference method converges if and only if it is stable.

Using Definition 2.1, we note that the method is consistent since the truncation errors in the approximations for the Caputo derivative (Eq. (42)) and the space derivatives both go to zero as the step sizes τ, Δx and Δy go to zero, and therefore the trucation errors in the implicit fractional FTCS method also go to zero.

In discussing the errors in the proof of stability, we will use $\phi^n_{i,j}$ to mean the exact solution of (46) and (47) and $\widehat{\phi}^n_{i,j}$ to mean an approximate computed solution of (46) and (47) at a mesh point (x_i,y_j,t^n). Then, we can write the error as

$$\begin{aligned}e^n_{i,j}=\phi^n_{i,j}-\widehat{\phi}^n_{i,j},\ i=0,1,2,\ldots,N_1;\ j=0,1,2,\ldots,N_2;\\ n=0,1,2,\ldots,N.\end{aligned}\tag{48}$$

We will assume that there is an initial "machine error" in the initial conditions of $e^0_{i,j}=\psi(x_i,y_j)-\widehat{\phi}^0_{i,j}$. We will now prove that solving the discretized equations by iteration for $n=0,1,2,\ldots,N$ is a stable process. From (46) and (47), we have

$$\begin{aligned}&(P_1-P_2)e^1_{i+1,j}-(P_1+P_2)e^1_{i-1,j}\\&\quad+[1+2P_2+2P_3+\tau^\alpha\Gamma(2-\alpha)R]e^1_{i,j}\\&\quad-P_3(e^1_{i,j+1}+e^1_{i,j-1})\\&=e^0_{i,j},\end{aligned}\tag{49}$$

$$\begin{aligned}&(P_1-P_2)e^{n+1}_{i+1,j}-(P_1+P_2)e^{n+1}_{i-1,j}\\&\quad+[1+2P_2+2P_3+\tau^\alpha\Gamma(2-\alpha)R]e^{n+1}_{i,j}\\&\quad-P_3(e^{n+1}_{i,j+1}+e^{n+1}_{i,j-1})\\&=(b_0-b_1)e^n_{i,j}+\sum_{s=1}^{n-1}(b_s-b_{s+1})e^{n-s}_{i,j}+b_ne^0_{i,j},\end{aligned}\tag{50}$$

which can be written in matrix form as

$$\begin{cases}A\mathbf{E}^1=\mathbf{E}^0,\\ A\mathbf{E}^{n+1}=(b_0-b_1)\mathbf{E}^n+(b_1-b_2)\mathbf{E}^{n-1}+\cdots\\ \qquad\qquad +(b_{n-1}-b_n)\mathbf{E}^1+b_n\mathbf{E}^0,\\ \mathbf{E}^0,\end{cases}\tag{51}$$

where

$$\mathbf{E}^n=\begin{bmatrix}\mathbf{E}^n_1\\ \mathbf{E}^n_2\\ \vdots\\ \mathbf{E}^n_{N_1-1}\end{bmatrix}\ \text{and}\ \mathbf{E}^n_i=\begin{bmatrix}e^n_{i,1}\\ e^n_{i,2}\\ \vdots\\ e^n_{i,N_2-1}\end{bmatrix},\ i=1,2,\ldots,N_1,\tag{52}$$

and where $A = [A_{i,j}]$ is the matrix of coefficients in Eq. (50). Since these matrices can be very big and the coefficients can be easily obtained from Eq. (45) or (50), we will not give them here.

Then, the following result can be proved using mathematical induction.

Theorem 3.1: $||\mathbf{E}^n||_\infty \leq ||\mathbf{E}^0||_\infty,\ n = 1, 2, 3, \ldots.$

Proof: We first note that the coefficients $P_1, P_2, P_3 > 0$ and that the step sizes Δx and τ can be chosen so that $P_1 \leq P_2$. Then, by definition of infinity norm,

$$\|\mathbf{E}^n\|_\infty = \max_{1\leq i\leq N_1-1;\ 1\leq j\leq N_2-1} |e^n_{i,j}|. \tag{53}$$

Next, we define

$$\begin{aligned} |e^1_{p,q}| &= \max_{1\leq i\leq N_1-1;\ 1\leq j\leq N_2-1} |e^1_{i,j}| \\ &= \|\mathbf{E}^1\|_\infty \end{aligned} \tag{54}$$

and then, since

$$\begin{aligned} &(P_1 - P_2) - (P_1 + P_2) + [1 + 2P_2 + 2P_3 + \tau^\alpha\Gamma(2-\alpha)R] \\ &-2P_3 - \tau^\alpha\Gamma(2-\alpha)R = 1, \end{aligned} \tag{55}$$

we have from (49) that

$$\begin{aligned} |e^1_{p,q}| &= \big\{(P_1 - P_2) - (P_1 + P_2) \\ &\quad +[1 + 2P_2 + 2P_3 + \tau^\alpha\Gamma(2-\alpha)R] \\ &\quad -2P_3 - \tau^\alpha\Gamma(2-\alpha)R\big\}|e^1_{p,q}| \\ &= (P_1 - P_2)|e^1_{p,q}| - (P_1 + P_2)|e^1_{p,q}| \\ &\quad +[1 + 2P_2 + 2P_3 + \tau^\alpha\Gamma(2-\alpha)R]|e^1_{p,q}| \\ &\quad -P_3(|e^1_{p,q}| + |e^1_{p,q}|) - \tau^\alpha\Gamma(2-\alpha)R|e^1_{p,q}| \\ &\leq (P_1 - P_2)|e^1_{p+1,q}| - (P_1 + P_2)|e^1_{p-1,q}| \\ &\quad +[1 + 2P_2 + 2P_3 + \tau^\alpha\Gamma(2-\alpha)R]|e^1_{p,q}| \\ &\quad -P_3(|e^1_{p,q+1}| + |e^1_{p,q-1}|) \\ &\leq \Big|(P_1 - P_2)e^1_{p+1,q} - (P_1 + P_2)e^1_{p-1,q} \\ &\quad +[1 + 2P_2 + 2P_3 + \tau^\alpha\Gamma(2-\alpha)R]e^1_{p,q} \\ &\quad -P_3(e^1_{p,q+1} + e^1_{p,q-1})\Big| \\ &= |e^0_{p,q}| \leq \|\mathbf{E}^0\|_\infty, \end{aligned} \tag{56}$$

and therefore

$$\|\mathbf{E}^1\|_\infty = |e^1_{p,q}\| \leq \|\mathbf{E}^0\|_\infty. \tag{57}$$

We now prove that if

$$\|\mathbf{E}^s\|_\infty \leq \|\mathbf{E}^0\|_\infty,\ s = 1, 2, \ldots, n \tag{58}$$

then

$$\|\mathbf{E}^s\|_\infty \leq |\mathbf{E}^0\|_\infty,\ s = 1, 2, \ldots, n+1 \tag{59}$$

Letting

$$|e^{n+1}_{p,q}| = \|\mathbf{E}^{n+1}\|_\infty = \max_{1\leq i\leq N_1-1;1\leq j\leq N_2-1} |e^{n+1}_{i,j}|, \tag{60}$$

we have from (49) and (50) and using Lemma 3.1 that

$$\begin{aligned} |e^{n+1}_{p,q}| &= (P_1 - P_2)|e^{n+1}_{p,q}| - (P_1 + P_2)|e^{n+1}_{p,q}| \\ &\quad +[1 + 2P_2 + 2P_3 + \tau^\alpha\Gamma(2-\alpha)R]|e^{n+1}_{p,q}| \\ &\quad -P_3(|e^{n+1}_{p,q}| + |e^{n+1}_{p,q}|) \\ &\quad -\tau^\alpha\Gamma(2-\alpha)R|e^{n+1}_{p,q}| \\ &\leq (P_1 - P_2)|e^{n+1}_{p+1,q}| - (P_1 + P_2)|e^{n+1}_{p-1,q}| \\ &\quad +[1 + 2P_2 + 2P_3 + \tau^\alpha\Gamma(2-\alpha)R]|e^{n+1}_{p,q}| \\ &\quad -P_3(|e^{n+1}_{p,q+1}| + |e^{n+1}_{p,q-1}|) \\ &\leq \Big|(P_1 - P_2)e^{n+1}_{p+1,q} - (P_1 + P_2)e^{n+1}_{p-1,q} \\ &\quad +[1 + 2P_2 + 2P_3 + \tau^\alpha\Gamma(2-\alpha)R]e^{n+1}_{p,q} \\ &\quad -P_3(e^{n+1}_{p,q+1} + e^{n+1}_{p,q-1})\Big| \\ &= \Big|(b_0 - b_1)e^n_{p,q} + \sum_{s=1}^{n-1}(b_s - b_{s+1})e^{n-s}_{p,q} \\ &\quad +b_n e^0_{p,q}\Big| \\ &\leq (b_0 - b_1)|e^n_{p,q}| + \sum_{s=1}^{n-1}(b_s - b_{s+1})|e^{n-s}_{p,q}| \\ &\quad +b_n|e^0_{p,q}| \\ &\leq (b_0 - b_1)\|\mathbf{E}^n\|_\infty \\ &\quad +\sum_{s=1}^{n-1}(b_s - b_{s+1})\|\mathbf{E}^{n-s}\|_\infty + b_n\|\mathbf{E}^0|_\infty \\ &\leq \{b_0 - b_1 + \sum_{s=1}^{n-1}(b_s - b_{s+1}) + b_n\}|\mathbf{E}^0|_\infty \\ &= \|\mathbf{E}^0\|_\infty, \end{aligned} \tag{61}$$

since $b_0 - b_1 + \sum_{s=1}^{n-1}(b_s - b_{s+1}) + b_n = b_0 = 1$.

Therefore, we have proved that if

$$\|\mathbf{E}^s\|_\infty = |e^s_{p,q}| \leq \|\mathbf{E}^0|_\infty,\quad s = 1, 2, \ldots, n \tag{62}$$

then

$$\|\mathbf{E}^{n+1}\|_\infty = |e^{n+1}_{p,q}| \leq \|\mathbf{E}^0|_\infty \tag{63}$$

Therefore, since we have proved that $\|\mathbf{E}^1\|_\infty \leq \|\mathbf{E}^0|_\infty$, we have proved by induction that

$$\|\mathbf{E}^n\|_\infty \leq \|\mathbf{E}^0|_\infty, n = 1, 2, \ldots, N. \tag{64}$$

Hence, the following theorem has been proved. ■

Theorem 3.2: The implicit difference approximation defined by Eq. (45) is stable if the step sizes satisfy the inequality $P_1 = \frac{u\tau^\alpha\Gamma(2-\alpha)}{2\Delta x} \leq \frac{\varepsilon\tau^\alpha\Gamma(2-\alpha)}{(\Delta x)^2} = P_2$.

Therefore, since the error equation is stable the errors in the numerical solution by the implicit fractional FTCS method will be bounded by the initial "machine error".

We note here that the first and second authors have derived an explicit proof that the exact solution of the discretized equations (45) converge to the exact solution of the partial differential equations (33)–(35) in the limit as the step sizes $\tau, \Delta x, \Delta y \to 0$. However, we will not include the proof in this paper.

IV. Numerical Results

A. Integer-order

In this section, the implicit FTCS finite difference method is used to obtain numerical solutions for the following cases

(homogeneous and nonhomogeneous) of three-dimensional ADRE problems of air pollution. All programs for the numerical solutions have been written in Matlab.

Problem 1: We solve an air pollution model for a tunnel of length L (x direction), width W (y direction) and height H (z direction) corresponding to the ADRE in Eq. (7), where $\Phi = \Phi(x, y, z, t)$ [kg/m^3] is the air pollutant concentration at (x, y, z) [m] and time t [s], (u, v, w) are wind velocity components [m/s] in (x, y, z) directions, D_x and D_y are constant diffusion coefficients in the horizontal direction [m^2/s], D_z is a constant diffusion coefficient in the $z-$direction (vertical) [m^2/s], R is a reaction coefficient, and $Q(x, y, z, t)$ is the rate of change of concentrations of sources or sinks of air pollutants [kg/m^3·s].

Then, using the results for the implicit FTCS method from section II-A the corresponding FTCS equation is the same as Eq. (11).

For the air pollution models, we assume that the initial condition is

$$\Phi(x, y, z, 0) = 0, \quad 0 \le x \le 1;\ 0 \le y \le 1;\ 0 \le z \le 1, \tag{65}$$

and that the boundary conditions are as shown in Table I.

TABLE I
BOUNDARY CONDITIONS

Boundary	Boundary condition	Value
Entrance gate : $x = 0,\ 0 \le y < 0.5,\ 0 \le z \le 1$	$\Phi(0, y, z, t)$	0
Entrance gate : $x = 0,\ 0.5 \le y \le 1,\ 0 \le z \le 1$	$\Phi(0, y, z, t)$	1
Exit gate : $x = 1, 0 \le y \le 1,\ 0 \le z \le 1$	$\frac{\partial \Phi}{\partial x}(1, y, z, t)$	0
Right side wall : $0 \le x < 0.3,\ y = 0,\ 0 \le z \le 1$	$\Phi(x, 0, z, t)$	0
Right side wall : $0.3 \le x \le 0.6,\ y = 0,\ 0 \le z \le 1$	$\Phi(x, 0, z, t)$	1
Right side wall : $0.6 < x \le 1,\ y = 0,\ 0 \le z \le 1$	$\Phi(x, 0, z, t)$	0
Left side wall : $0 < x < 1,\ y = 1,\ 0 \le z \le 1$	$\frac{\partial \Phi}{\partial y}(x, 1, z, t)$	0
Ground : $0 < x < 1,\ 0 < y < 1,\ z = 0$	$\frac{\partial \Phi}{\partial z}(x, y, 0, t)$	0
Ceiling : $0 < x < 1,\ 0 < y < 1,\ z = 1$	$\frac{\partial \Phi}{\partial z}(x, y, 1, t)$	0

Case 1 : We consider the 3D ADRE (7). By taking $w = 0, R = 0, Q = 0, L = 1, W = 1$ and $H = 1$, Eq. (7) reduces to the following 2D advection 3D diffusion equation for transport of pollutants in the street tunnel problem discussed in [42], [49].

$$\frac{\partial \Phi}{\partial t} + u\frac{\partial \Phi}{\partial x} + v\frac{\partial \Phi}{\partial y} - D_x\frac{\partial^2 \Phi}{\partial x^2} - D_y\frac{\partial^2 \Phi}{\partial y^2} - D_z\frac{\partial^2 \Phi}{\partial z^2} = 0, \qquad 0 < t < T. \tag{66}$$

This partial differential equation with initial condition (65) and boundary conditions in Table I comes from a model of pollution distribution in a street tunnel where there is a steady wind flowing in the x and y directions and there is no pollutant flow through the solid side-walls or the solid base and roof of the tunnel. We use the nondimensionalised parameters $\Delta x = \Delta y = \Delta z = 0.1, \Delta t = 0.005, D_x = D_y = D_z = 0.5, u = 0.6, v = 0.4$ and time $T = 20$.

The numerical solutions and the contour plots of the problem obtained using the implicit FTCS scheme in Eq. (11) are plotted in Figs. 1 and 2. We have tested the accuracy of our numerical solutions by comparing them with those of Kusuma et al. [42] and found that there was good agreement. It can be seen from the contour plots that the qualitative behaviors in the plots are similar for all diffusion coefficient values, but that there are considerable differences in detail. In particular, an increase in the diffusion coefficient gives, as expected, a more uniform spread of the pollution.

Case 2: In this problem, we consider the three-dimensional advection-diffusion-reaction equation in Eq. (7) for the special case of advection only in the horizontal directions, i.e., for $w = 0$. Otherwise, the meaning of all symbols is the same as described above.

This case of partial differential equation and initial condition (65) and boundary conditions in Table I comes from a model of pollution distribution in a street tunnel where there is a steady wind blowing in the x and y directions and there is no flux of pollutant through the solid side-walls or the solid base and roof of the tunnel. In the numerical simulations, we use the nondimensionalised parameters $\Delta x = \Delta y = \Delta z = 0.1, \Delta t = 0.005, D_x = D_y = D_z = 0.2, u = 0.6, v = 0.4$ and time $T = 20$.

We have computed the numerical solutions of this model using the implicit FTCS method for the following cases. The plots of the numerical solutions for the cases below are qualitatively very similar to the plots in Fig. 1 and therefore we will not repeat them.

1) $R = 0.05$ and $Q = 0.007$. The contour plot for this case is shown in Fig. 3 at a height $z = 0.2$ meters.
2) $R = 0.5$ and $Q = -e^{-t}$. The contour plot for this case is shown in Fig. 4 at a height $z = 0.2$ meters.

It can be seen from the contour plots in Figs. 3 and 4 that the solutions for the different Q and R values show similar qualitative behavior but with differences in detail.
Finally, we show numerical solutions for $z = 0.2$ m for $Q = 0.007$ and $R = 0.05, 0.1, 0.5$. The 2D plots for this case are shown in Figs. 5 (a) at $y = 0.5$ m and (b) at $x = 0.5$ m.

It can be clearly seen from Fig. 5 that at the value of $Q = 0.007$ there is a marked decrease in pollution as the value of the reaction coefficient R is increased.

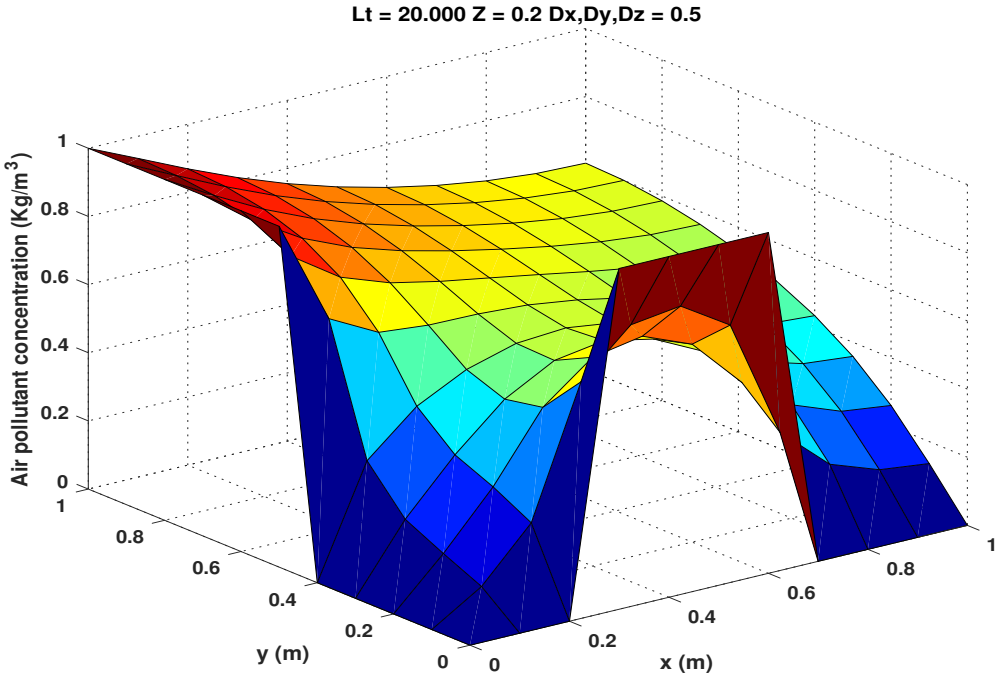

Fig. 1. Pollutant distribution for Problem 1 Case 1 in a street tunnel with advection only in x and y directions ($u = 0.6, v = 0.4$) at $z = 0.2$ m for a range of diffusion coefficients $D = D_x = D_y = D_z = 0.5$

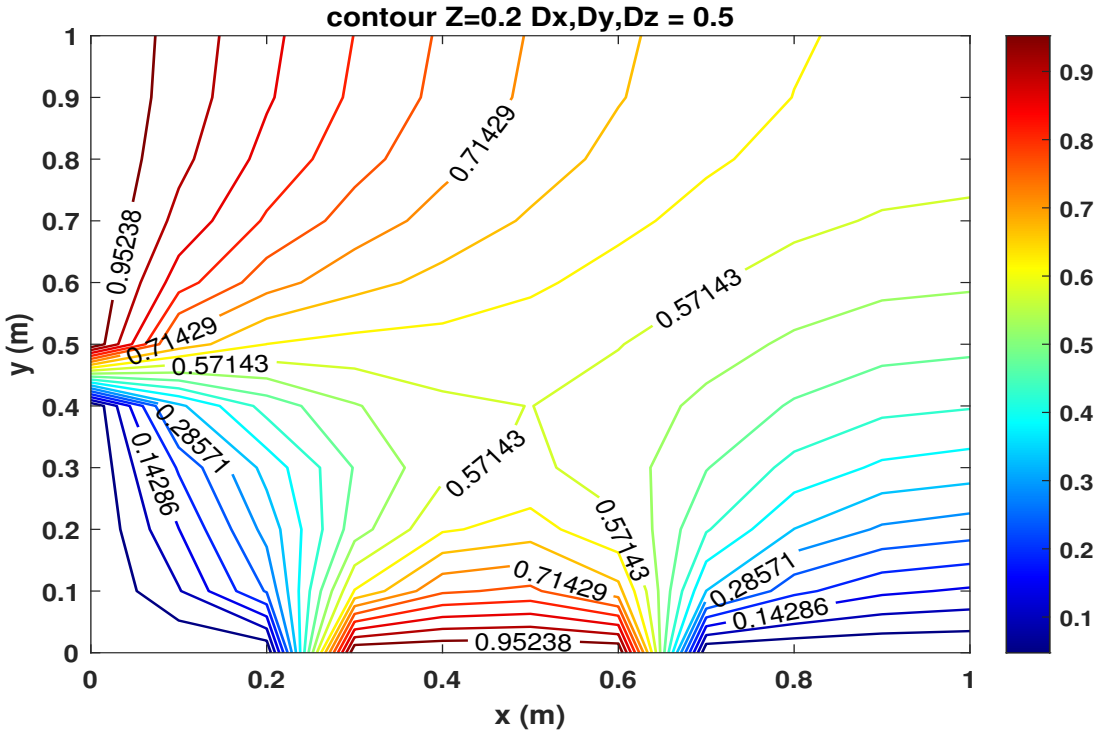

Fig. 2. Contour plots of air pollutant concentration for Problem 1 Case 1 in a street tunnel with advection only in x and y directions ($u = 0.6, v = 0.4$) at $z = 0.2$ m for a range of diffusion coefficients $D = D_x = D_y = D_z = 0.5$

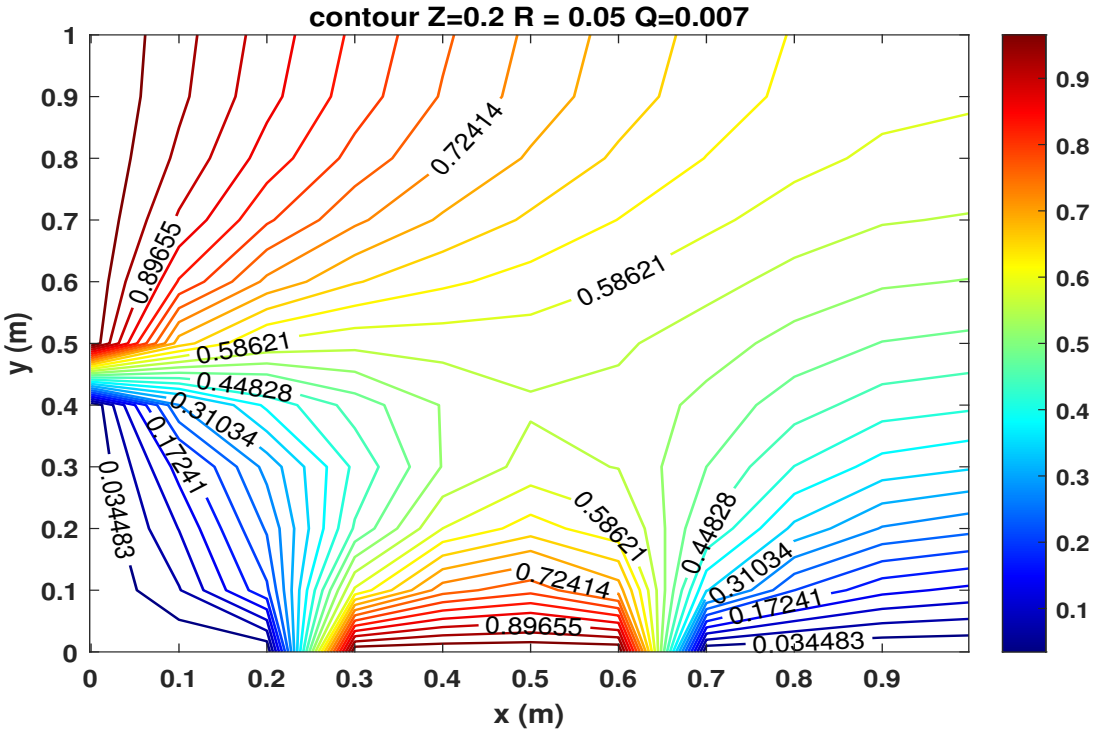

Fig. 3. Contour plots of air pollutant concentration in the (x, y) plane for Problem 1 Case 2 at $z = 0.2$ m for $R = 0.05$ and $Q = 0.007$

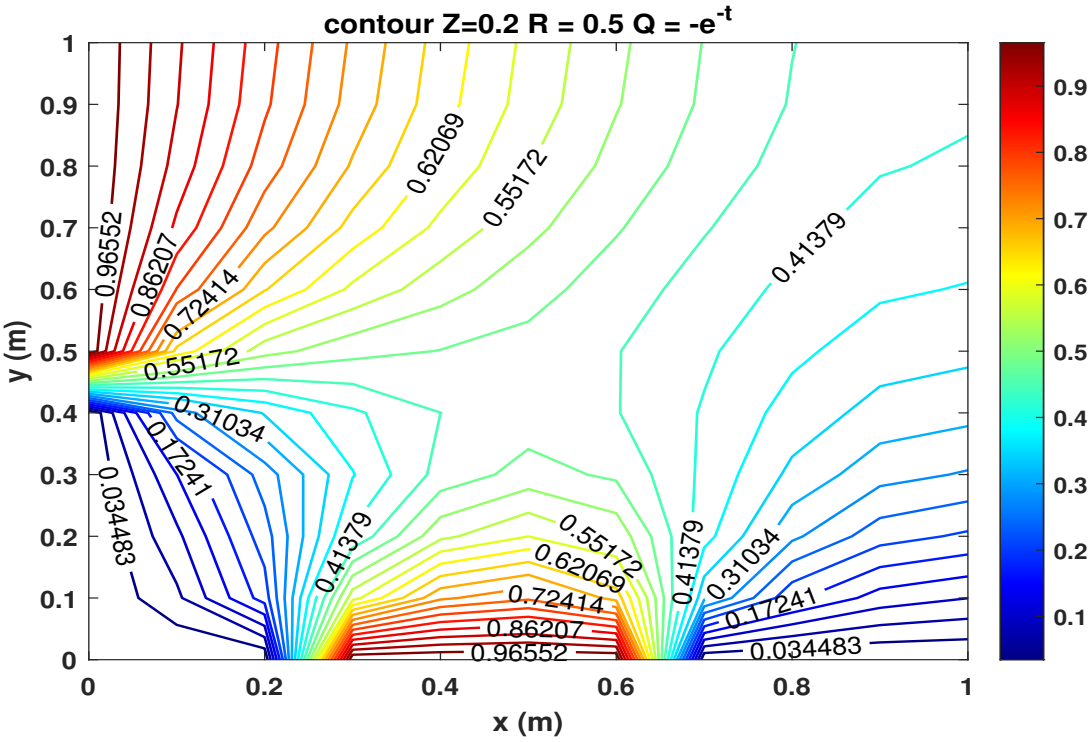

Fig. 4. Contour plot of air pollutant concentration in the (x, y) plane for Problem 1 Case 2 at $z = 0.2$ m for $R = 0.5$ and $Q = -e^{-t}$

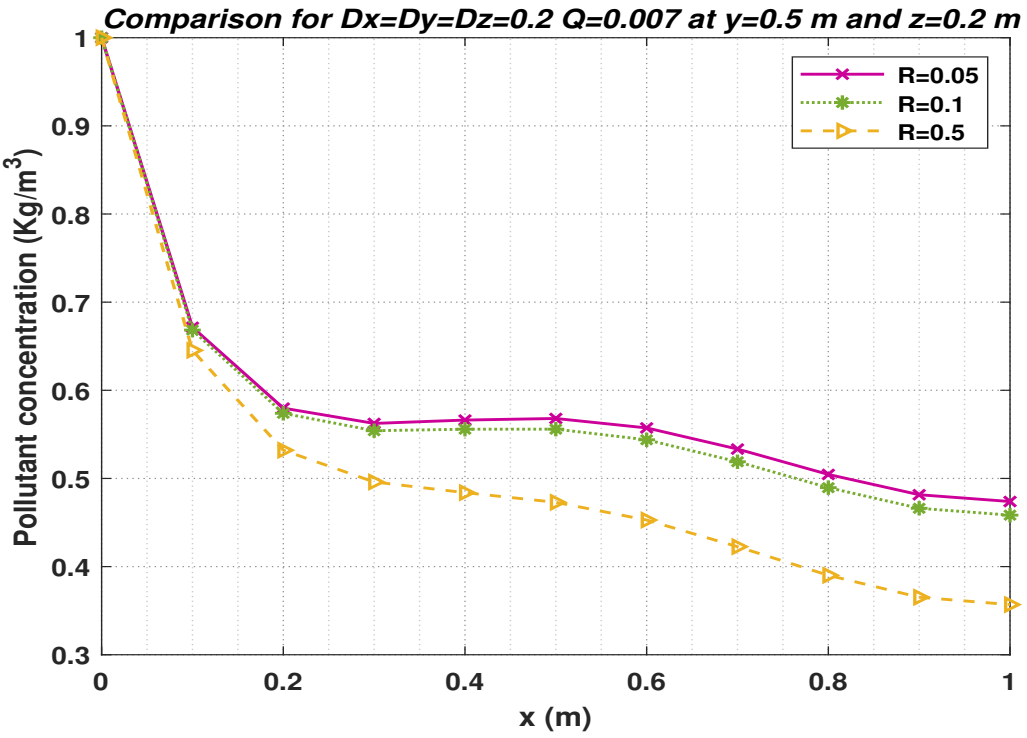

(a)

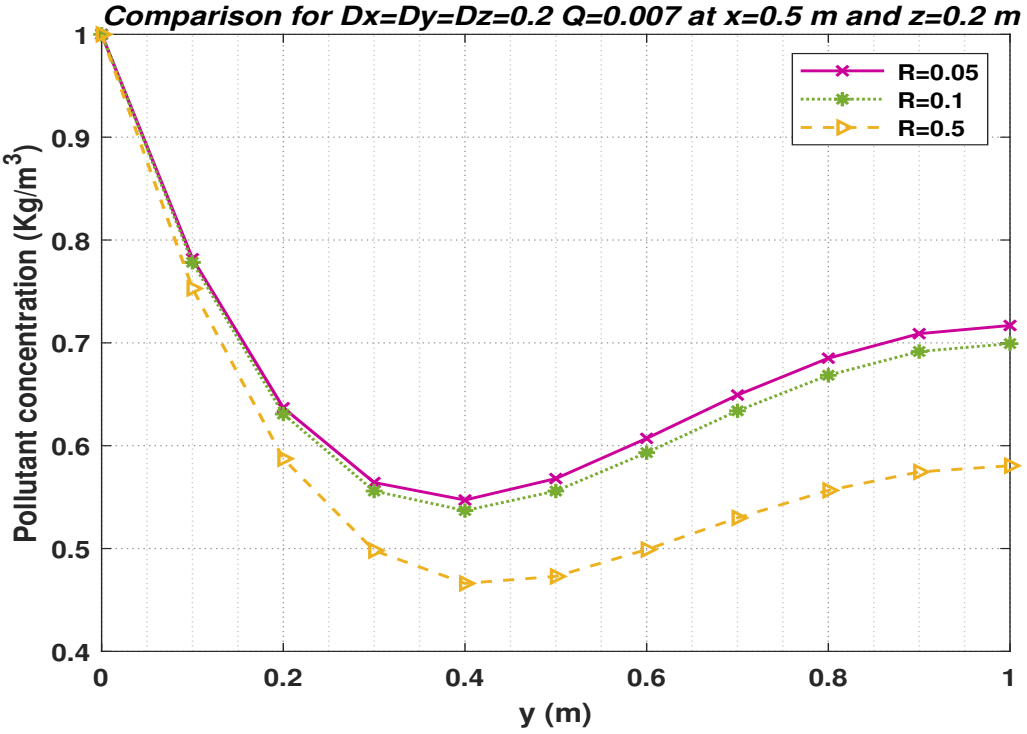

(b)

Fig. 5. Comparison of numerical solutions for Problem 1 Case 2 at $z = 0.2$ m for $Q = 0.007$ of $R = 0.05, 0.1, 0.5$ at (a) $y = 0.5$ m and (b) $x = 0.5$ m

Problem 2: In this problem, we consider an advection-diffusion model of air pollution in a tunnel with air flow in the x and y directions, diffusion in x, y and z directions, but with no reaction or source terms. The three-dimensional advection-diffusion-reaction equation with $w = 0, R = 0, Q = 0$ can then be written as [50]

$$\frac{\partial C}{\partial t} + u\frac{\partial C}{\partial x} + v\frac{\partial C}{\partial y} = D_x\frac{\partial^2 C}{\partial x^2} + D_y\frac{\partial^2 C}{\partial y^2} + D_z\frac{\partial^2 C}{\partial z^2}. \tag{67}$$

In this model, the length is $L = 192$ meters, the width is $W = 26$ meters and an entrance gate in the right-hand side wall has been added to allow air flow in the y direction. We assume $\Delta x = \Delta y = \Delta z = 2$ m, $\Delta t = 0.06$ sec, $D_x = D_y = 0.1592$ m^2/sec, $D_z = 0.05$ m^2/sec, $u = 2.7778$ m/sec, and $v = \frac{u}{20}$ m/sec.

The initial condition is

$$C(x, y, z, 0) = 0, \quad 0 \le x \le 192;\ 0 \le y \le 26;\ 0 \le z \le 6, \tag{68}$$

and the boundary conditions are shown in Table II.

TABLE II
BOUNDARY CONDITIONS FOR PROBLEM 2

Boundary	Boundary condition	Value
Entrance gate ($x = 0$) : $x = 0,\ 0 < y < 26,\ 0 < z < 6$	$C(0, y, z, t)$	1
Exit gate : $x = 192, 0 < y < 26,\ 0 < z < 6$	$\frac{\partial C}{\partial x}(192, y, z, t)$	-0.01
Right side wall : $0 < x < 64, 129 < x < 192,\ y = 0,$ $0 < z < 6$	$C(x, 0, z, t)$	0
Right side wall gap : $64 \le x \le 129,\ y = 0,\ 0 < z < 6$	$C(x, 0, z, t)$	0.5
Left side wall : $0 < x < 192,\ y = 26,\ 0 < z < 6$	$\frac{\partial C}{\partial y}(x, 26, z, t)$	0
Ground : $0 < x < 192,\ 0 < y < 26,\ z = 0$	$\frac{\partial C}{\partial z}(x, y, 0, t)$	0
Platform ceiling : $0 < x < 192,\ 4 < y < 17,\ z = 6$	$\frac{\partial C}{\partial z}(x, y, 6, t)$	0
Ceiling parallel gaps : $0 < x < 192,\ 0 < y \le 4,$ $17 \le y < 26, z = 6$	$\frac{\partial C}{\partial z}(x, y, 6, t)$	-0.01

We have computed the air pollutant concentration levels for Problem 2 for the boundary conditions in Table II and plotted the results at $t = 30$ seconds and $t = 120$ seconds. The numerical solutions and contour plots at $t = 30$ seconds are shown in Fig. 6 (a) and (b) and at $t = 120$ seconds in Fig. 7 (a) and (b).

We have also examined the effect of changing the conditions on the left side wall ($y = 26$). The new conditions at $y = 26$ are as follows.

$$\text{Left side wall: } \frac{\partial C}{\partial y}(x, 26, z, t) = -0.25C(x, 26, z, t), \tag{69}$$

$$\text{Left side wall: } \frac{\partial C}{\partial y}(x, 26, z, t) = -0.5C(x, 26, z, t). \tag{70}$$

A comparison of the solutions for the original left side wall conditions in Table II and the conditions in Eqs. (69) and (70) are shown in Fig. 8 at $z = 4$ m and $t = 120$ s for $y = 26$ m. It can be seen that the effects of changing the boundary conditions at the left side wall decrease rapidly as the distance from the wall increases.

B. Fractional-order

We use the implicit FTCS scheme to solve the Caputo fractional-time version of ADRE. We will consider both the one-dimensional and the two-dimensional case. The two-dimensional model is as follows.

$$\frac{\partial^\alpha \phi(\mathbf{x}, t)}{\partial t^\alpha} + \bar{u}\frac{\partial \phi(\mathbf{x}, t)}{\partial x} - D_x\frac{\partial^2 \phi(\mathbf{x}, t)}{\partial x^2} - D_y\frac{\partial^2 \phi(\mathbf{x}, t)}{\partial y^2} + R\phi(\mathbf{x}, t) = Q(\mathbf{x}, t),$$
$$\mathbf{x} = (x, y) \in (0, L_1) \times (0, L_2),\ t \in (0, T], \tag{71}$$

where $\frac{\partial^\alpha \phi(\mathbf{x},t)}{\partial t^\alpha}$ is the Caputo fractional-order time derivative of order α, and D_x, D_y are diffusion coefficients, R is the reaction term and $Q(\mathbf{x}, t)$ is the source term.

The implicit difference equation approximation (FDM) is

$$\begin{aligned}(P_1 - P_2)\phi_{i+1,j}^{n+1} - (P_1 + P_2)\phi_{i-1,j}^{n+1} + \big[1 + 2P_2 + 2P_3 \\ + \tau^\alpha\Gamma(2-\alpha)R\big]\phi_{i,j}^{n+1} - P_3(\phi_{i,j+1}^{n+1} + \phi_{i,j-1}^{n+1}) \\ = \phi_{i,j}^{n} - \sum_{s=1}^{n} b_s\left(\phi_{i,j}^{n+1-s} - \phi_{i,j}^{n-s}\right) + \tau^\alpha\Gamma(2-\alpha)Q_{i,j}^{n+1},\end{aligned} \tag{72}$$

where

$$\begin{aligned}P_1 &= \frac{\bar{u}\tau^\alpha\Gamma(2-\alpha)}{2\Delta x}, \quad P_2 = \frac{D_x\tau^\alpha\Gamma(2-\alpha)}{(\Delta x)^2}, \\ P_3 &= \frac{D_y\tau^\alpha\Gamma(2-\alpha)}{(\Delta y)^2}, \quad b_s = (s+1)^{1-\alpha} - s^{1-\alpha}.\end{aligned} \tag{73}$$

After rearrangement, Eq. (72) can be written in the form

$$\begin{aligned}\phi_{i,j}^{n+1} + S_1\phi_{i-1,j}^{n+1} + S_2\phi_{i+1,j}^{n+1} + S_3(\phi_{i,j-1}^{n+1} + \phi_{i,j+1}^{n+1}) \\ = S_4\left(\phi_{i,j}^{n} - \sum_{s=1}^{n} b_s\left(\phi_{i,j}^{n+1-s} - \phi_{i,j}^{n-s}\right)\right) + S_5Q_{i,j}^{n},\end{aligned} \tag{74}$$

where

$$\begin{aligned}S_1 &= (-P_1 - P_2)/B, \quad S_2 = (P_1 - P_2)/B, \\ S_3 &= -P_3/B, \quad S_4 = 1/B, \\ S_5 &= (\tau^\alpha\Gamma(2-\alpha))/B,\end{aligned} \tag{75}$$

and

$$B = 1 + \frac{2D_x\Delta t}{(\Delta x)^2} + \frac{2D_y\Delta t}{\Delta y)^2} + \tau\Gamma(2-\alpha)R. \tag{76}$$

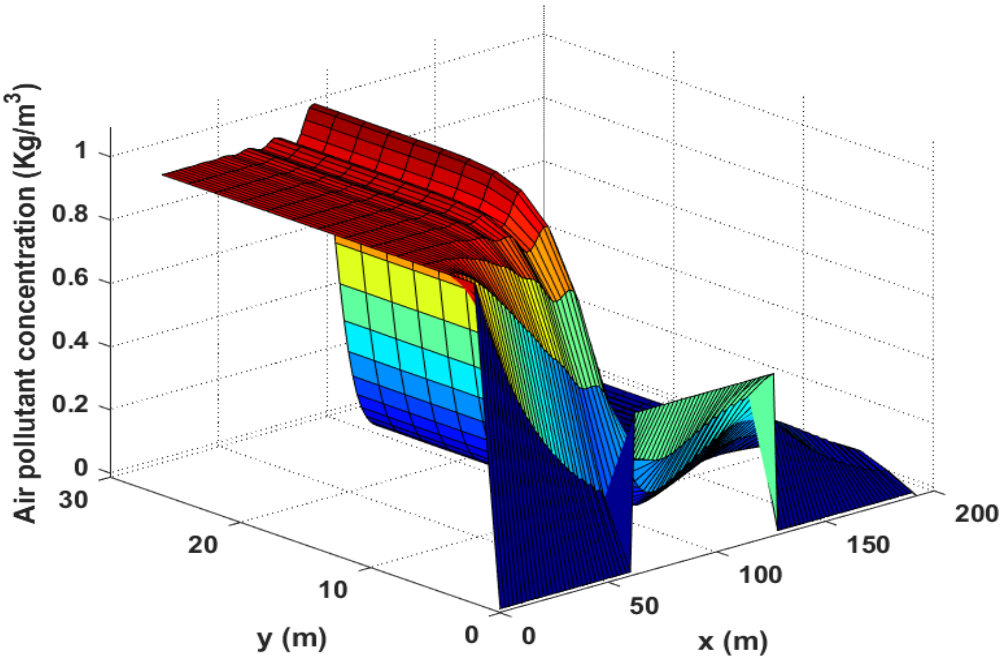

(a)

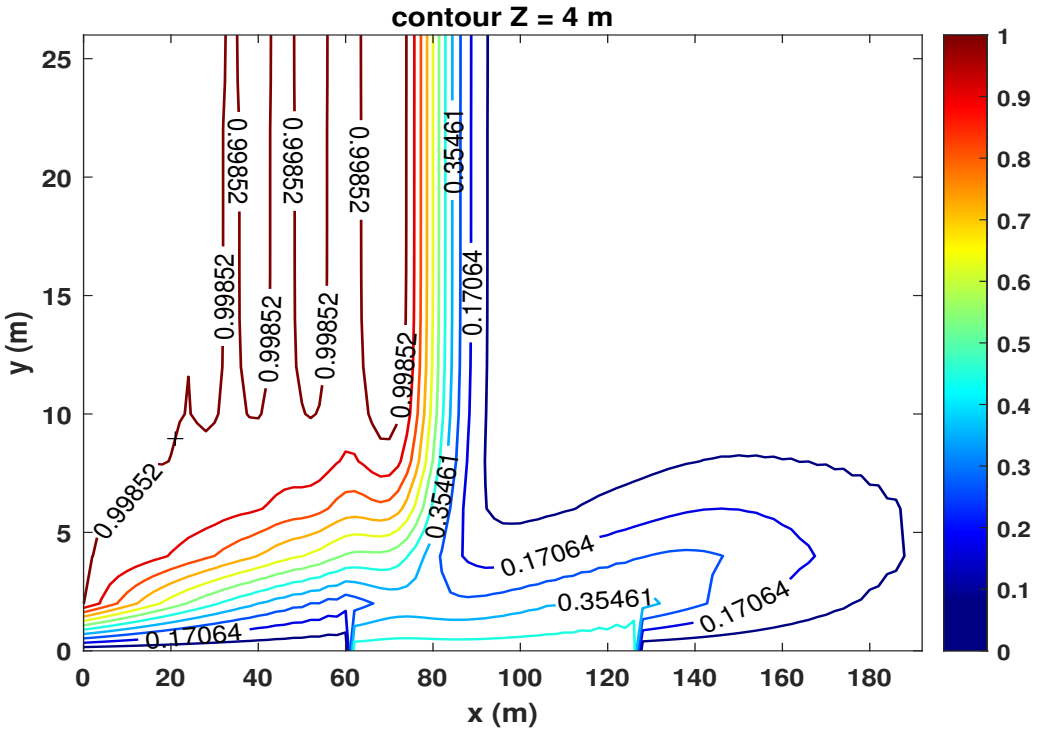

(b)

Fig. 6. Pollutant distribution and contour plot for Problem 2 with advection only in x and y directions at $z = 4$ m with left side wall boundary condition $\frac{\partial C}{\partial y}(x, 26, z, t) = 0$ at $t = 30$ sec

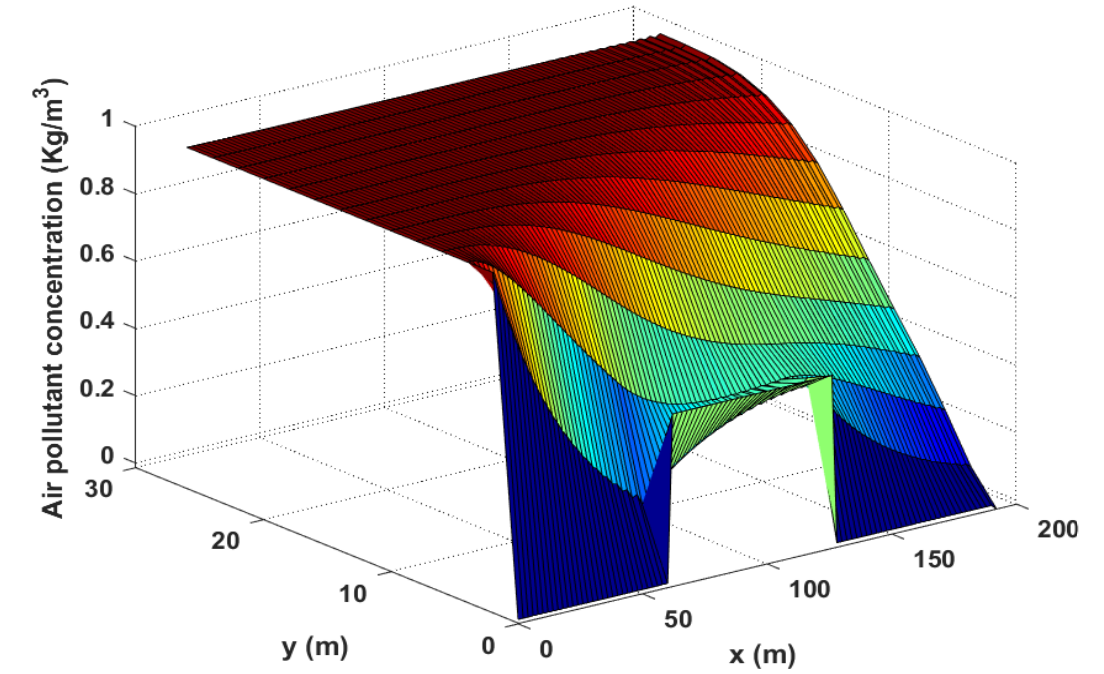

(a)

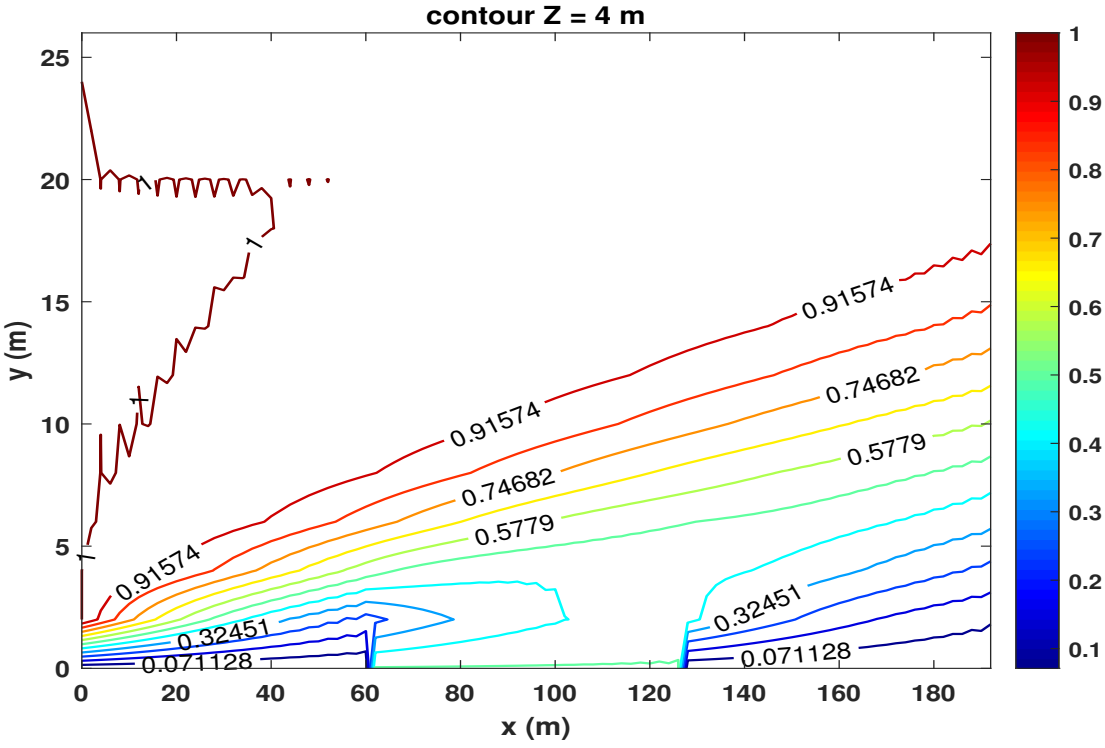

(b)

Fig. 7. Pollutant distribution and contour plot for Problem 2 with advection only in x and y directions at $z = 4$ m with left side wall boundary condition $\frac{\partial C}{\partial y}(x, 26, z, t) = 0$ at $t = 120$ sec

Problem 3: Consider the fractional time one dimensional advection-diffusion-reaction equation in Eq. (72) with $\bar{u} = 1, D_x = 1, D_y = 0, R = 0$ on $[0,1] \times [0,1]$ [51]

$$\frac{\partial^\alpha \phi}{\partial t^\alpha} + \frac{\partial \phi}{\partial x} - \frac{\partial^2 \phi}{\partial x^2} = Q. \tag{77}$$

The initial and boundary conditions are

$$\phi(x,0) = 0, \ x \in [0,1] \tag{78}$$

$$\phi(0,t) = 0, \quad \phi(1,t) = t^3, \ t \in (0,1], \tag{79}$$

where $0 < \alpha < 1$, and the source term is

$$Q(x,t) = \frac{6}{\Gamma(4-\alpha)} x^2 t^{3-\alpha} + 2t^3(x-1). \tag{80}$$

The exact solution of Eq. (77) is

$$\phi(x,t) = x^2 t^3. \tag{81}$$

After rearrangement, the implicit FTCS scheme of FDM from Eq. (74) can be written as

$$\begin{aligned} &\phi_{i,j}^{n+1} + S_1 \phi_{i-1,j}^{n+1} + S_2 \phi_{i+1,j}^{n+1} \\ &= S_3 \left(\phi_{i,j}^n - \sum_{s=1}^{n} b_s \phi_{i,j}^{n+1-s} + \sum_{s=1}^{n} b_s \phi_{i,j}^{n-s} \right), + S_4 Q_{i,j}^n, \end{aligned} \tag{82}$$

where

$$\begin{aligned} S_1 &= (-P1 - P2) \Big/ \left(1 + \frac{2D_x \Delta t}{(\Delta x)^2} \right), \\ S_2 &= (P1 - P2) \Big/ \left(1 + \frac{2D_x \Delta t}{(\Delta x)^2} \right), \\ S_3 &= 1 \Big/ \left(1 + \frac{2D_x \Delta t}{(\Delta x)^2} \right), \\ S_4 &= \tau^\alpha \Gamma(2-\alpha) \Big/ \left(1 + \frac{2D_x \Delta t}{(\Delta x)^2} \right). \end{aligned}$$

Figs. 9 (a)-(b) show a comparison of the numerical solution with the exact solution and maximum of absolute error, respectively. We assume that $\Delta t = 1/500$ and $\Delta x = 1/100$ for $\alpha = 0.1$ at $t = 0.5667, 0.9$ and 1. It can be seen that the errors between the exact solution and the computed solution are of order 10^{-3} at all times.

Problem 4: We consider the following two dimensional fractional time diffusion-reaction equation

$$\begin{aligned} &\frac{\partial^\alpha \phi(x,y,t)}{\partial t^\alpha} = D_x \frac{\partial^2 \phi}{\partial x^2} + D_y \frac{\partial^2 \phi}{\partial y^2} - R\phi + Q(x,y,t), \\ &(x,y) \in \Omega \times (0,T], \ \phi|_{\partial\Omega} = 0, \\ &\phi(x,y,0) = \sin \pi x \sin \pi y, \ (x,y) \in \Omega \end{aligned} \tag{83}$$

where $Q(x,y,t) = \frac{25 t^{1.6}}{12\Gamma(1-\alpha)}(t^2 + 2)\sin \pi x \sin \pi y, R = 0.01, \Omega = \{(x,y) | 0 < x < 1, 0 < y < 1\}$ and $\partial\Omega$ is the boundary of Ω.

After rearranging, the implicit FTCS scheme of Eq. (83) can be written as follows.

$$\begin{aligned} &\phi_{i,j}^{k+1} + P_1(\phi_{i+1,j}^{k+1} - \phi_{i-1,j}^{k+1}) + P_2(\phi_{i,j+1}^{k+1} + \phi_{i,j-1}^{k+1}) \\ &= P_3 \left(\phi_{i,j}^k - \sum_{s=1}^{k} b_s \phi_{i,j}^{k+1-s} + \sum_{s=1}^{k} b_s \phi_{i,j}^{k-s} \right) \\ &\quad + P_4 \left(\tau^\alpha \Gamma(2-\alpha) Q_{i,j}^{k+1} \right) \end{aligned} \tag{84}$$

where $b_s = (s+1)^{1-\alpha} - s^{1-\alpha}$

$$\begin{aligned} r_1 &= \frac{\tau^\alpha}{(\Delta x)^2}\Gamma(2-\alpha), \quad r_2 = \frac{\tau^\alpha}{(\Delta y)^2}\Gamma(2-\alpha), \\ P_1 &= -r_1/(1 + 2r_1 + 2r_2 + \tau^\alpha \Gamma(2-\alpha)R), \\ P_2 &= -r_2/(1 + 2r_1 + 2r_2 + \tau^\alpha \Gamma(2-\alpha)R), \\ P_3 &= 1/(1 + 2r_1 + 2r_2 + \tau^\alpha \Gamma(2-\alpha)R), \\ P_4 &= \tau^\alpha/(1 + 2r_1 + 2r_2 + \tau^\alpha \Gamma(2-\alpha)R). \end{aligned}$$

Comparisons of numerical solutions for $\alpha = 0.6, 0.7, 0.8$ and 0.9 with $R = 0.01$ and $R = 10$ are shown in Figs. 10 (a)-(b), respectively. It can be seen that $\alpha = 0.6$ gives the maximum of the solutions for the middle range of x values for both $R = 0.01$ and $R = 10$. Comparisons of numerical solutions for $R = 0.01$ and $R = 10$ are shown for $\alpha = 0.6, 0.7, 0.8$ and 0.9 in Figs. 11 (a)-(d), respectively. It can be seen that $R = 10$ gives a lower value of the solution ϕ than $R = 0.01$ for all values of α.

V. Conclusions

In this article, we have studied the implicit forward time central space (FTCS) finite difference method for solving integer-order three-dimensional advection-diffusion-reaction equations and for solving Caputo fractional-time two-dimensional advection-diffusion-reaction equations. We have proved consistency, stability and convergence of the integer-order method and consistency and stability for the fractional-order method. For the integer-order applications, we have solved 3-D air pollutant concentration problems for two cases of air pollution in traffic tunnels for a range of different source terms Q and reaction terms R. For case 1, we assumed that $Q = R = 0$, that there was advection in the x and y directions and diffusion in the x, y and z directions. We then compared our numerical solutions of $D_x = D_y = D_z = 0.2$ with previously published results of Kusuma et al. [42] and found that there was good agreement. For case 2, we considered that Q and R were non-zero, that there was advection in the x and y directions and diffusion in the x, y and z directions. We found that, as expected, an increase in diffusion resulted in a more uniform spread of pollution and that for a given pollution source Q an increase in the reaction term R increased the rate of reduction of the pollutant concentrations in the tunnel. For the integer-order method, we have shown that with suitable choices of time and space step sizes the implicit FTCS method is an efficient, accurate and convergent numerical method for solving 3D advection-reaction-diffusion equations. For the Caputo fractional-time method, we considered ADRE models for 1-D and 2-D problems and obtained numerical solutions using the implicit FTCS finite difference method. In the 1-D problems, good agreement was found between the numerical solutions and known exact solutions. For the 2-D problems, we assumed that $\alpha = 0.6, 0.7, 0.8, 0.9$ and $R = 0.01, 10$.

In a comparison of $\alpha = 0.6, 0.7, 0.8$ and 0.9 with $R = 0.01$ and $R = 10$, we found that $\alpha = 0.6$ gives the maximum of the solutions for the middle range of x values for both $R = 0.01$ and $R = 10$. For $R = 0.01$ and $R = 10$ with $\alpha = 0.6, 0.7, 0.8$ and 0.9, we found that $R = 10$ gives a lower value of the solution ϕ than $R = 0.01$ for all values of α.

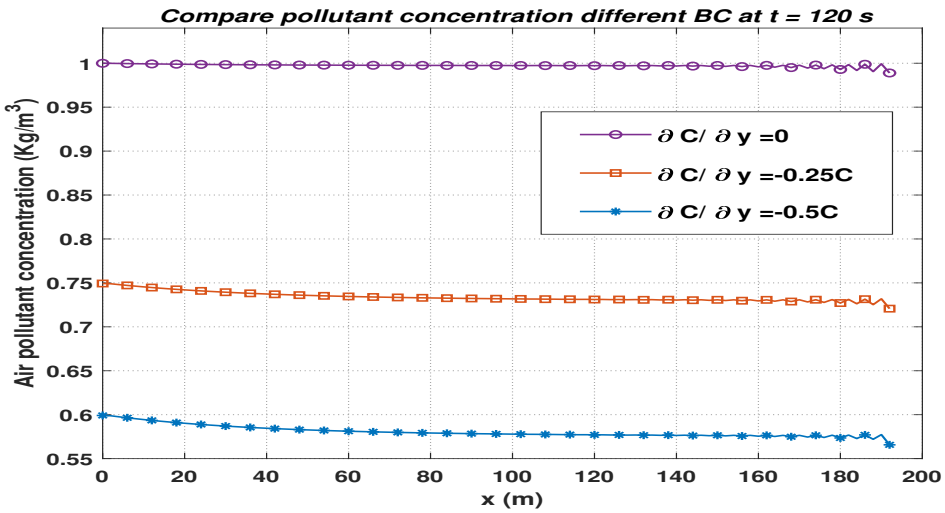

Fig. 8. Comparison of numerical solutions for Problem 2 at $z = 4$ m with the three different left side wall boundary conditions at $y = 26$ m at $t = 120$ sec

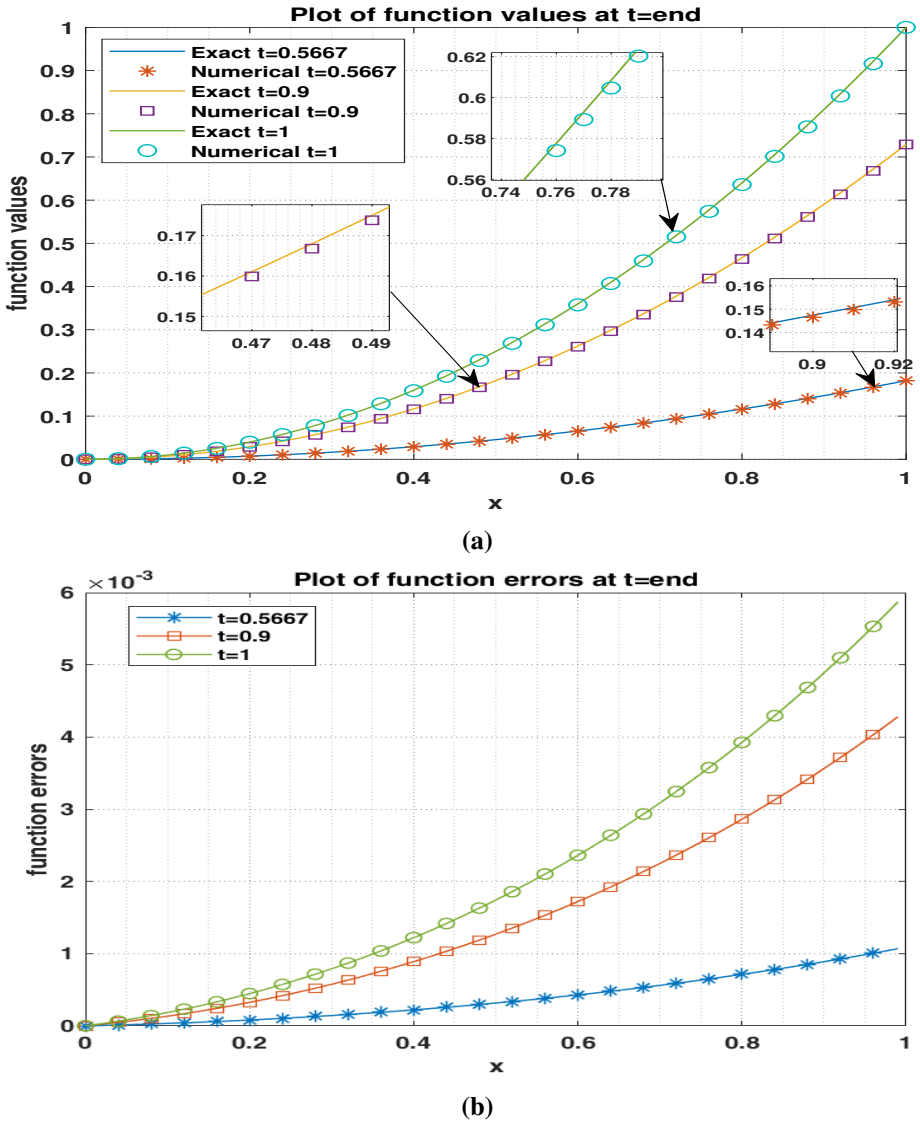

Fig. 9. Comparison of the numerical solution with the exact solution for fractional problem 3 for $\alpha = 0.1$ at times $t = 0.5667, 0.9$ and $t = 1$ for $\Delta t = 1/500, \Delta x = 1/100$

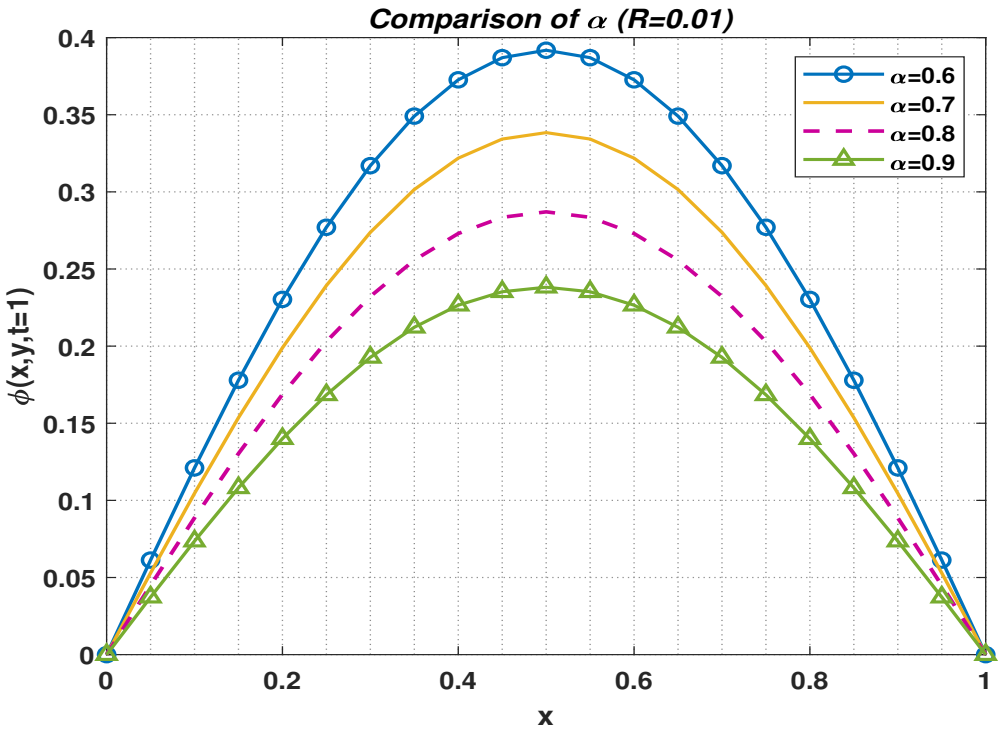

(a)

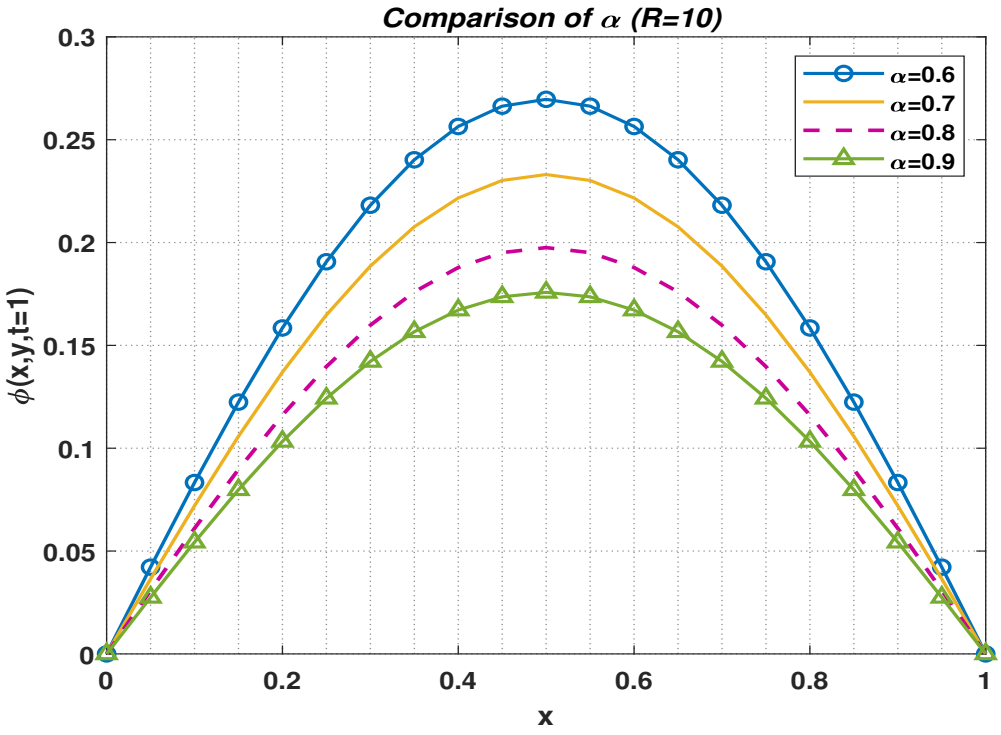

(b)

Fig. 10. Comparison of numerical solutions problem 4 for $\alpha = 0.6, 0.7, 0.8, 0.9$ at $y = 0.5, T = 1$ for (a) $R = 0.01$ and (b) $R = 10$

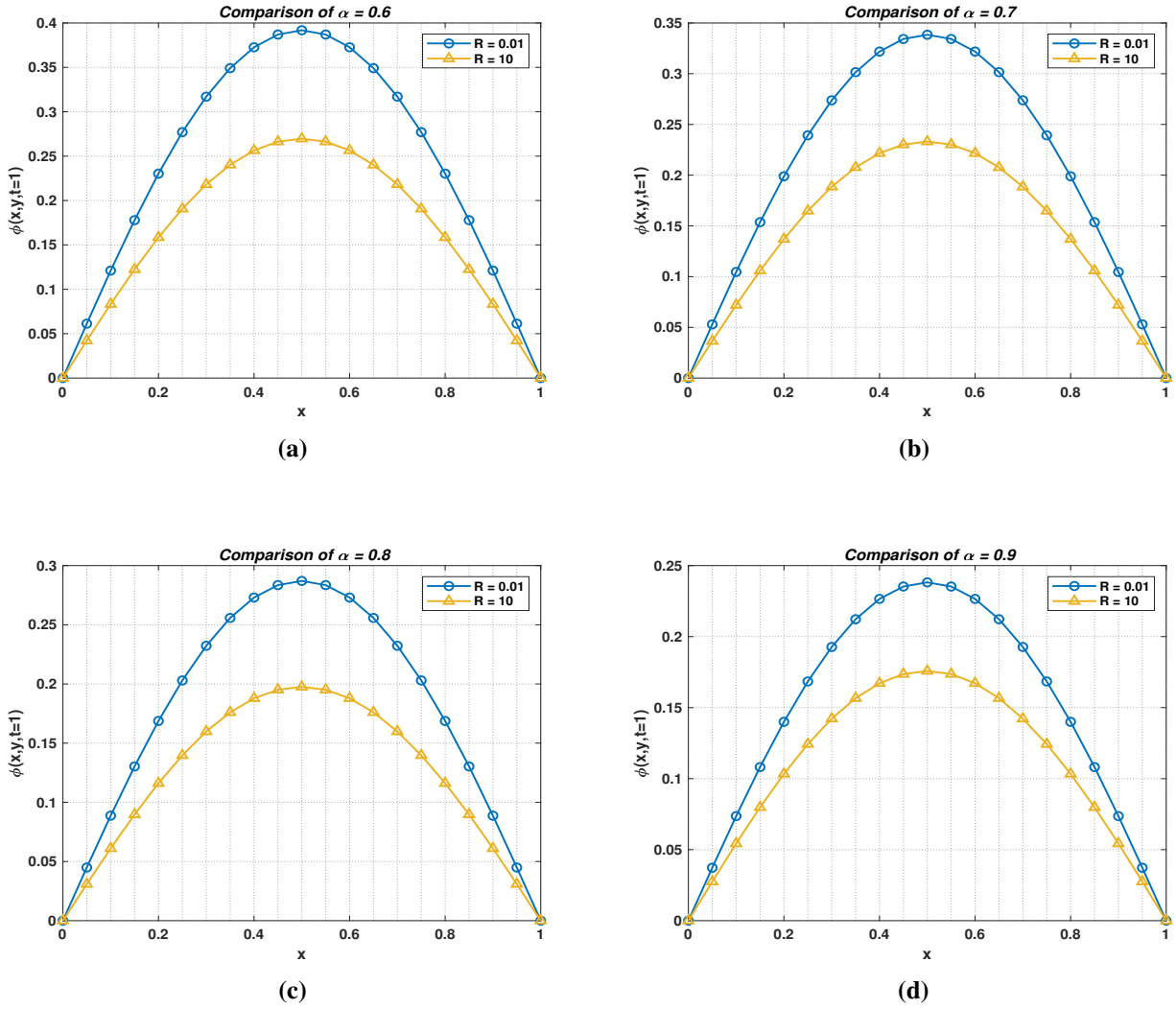

Fig. 11. Comparison of numerical solutions problem 4 at $y = 0.5, T = 1$ for $R = 0.01$ and $R = 10$ for (a) $\alpha = 0.6$, (b) $\alpha = 0.7$, (c) $\alpha = 0.8$ and (d) $\alpha = 0.9$

REFERENCES

[1] D. A. Garzón-Alvarado, C. Galeano, and J. Mantilla, "Computational examples of reaction–convection–diffusion equations solution under the influence of fluid flow: First example," *Applied Mathematical Modelling*, vol. 36, no. 10, pp. 5029–5045, 2012.

[2] S. Savović and A. Djordjevich, "Finite difference solution of the one-dimensional advection–diffusion equation with variable coefficients in semi-infinite media," *International Journal of Heat and Mass Transfer*, vol. 55, no. 15-16, pp. 4291–4294, 2012.

[3] A. R. Appadu and H. Gidey, "Time-splitting procedures for the numerical solution of the 2D advection-diffusion equation," *Mathematical Problems in Engineering*, vol. 2013, pp. 1–20, 2013.

[4] M. Bause and K. Schwegler, "Higher order finite element approximation of systems of convection–diffusion–reaction equations with small diffusion," *Journal of Computational and Applied Mathematics*, vol. 246, pp. 52–64, 2013.

[5] A. Mojtabi and M. O. Deville, "One-dimensional linear advection–diffusion equation: Analytical and finite element solutions," *Computers & Fluids*, vol. 107, pp. 189–195, 2015.

[6] A. Gharehbaghi, "Explicit and implicit forms of differential quadrature method for advection–diffusion equation with variable coefficients in semi-infinite domain," *Journal of Hydrology*, vol. 541, pp. 935–940, 2016.

[7] V. Gyrya and K. Lipnikov, "The arbitrary order mimetic finite difference method for a diffusion equation with a non-symmetric diffusion tensor," *Journal of Computational Physics*, vol. 348, pp. 549–566, 2017.

[8] E. Bahar and G. Gürarslan, "Numerical solution of advection-diffusion equation using operator splitting method," *International Journal of Engineering and Applied Sciences*, vol. 9, no. 4, pp. 76–88, 2017.

[9] M. A. Al-Jawary, M. M. Azeez, and G. H. Radhi, "Analytical and numerical solutions for the nonlinear Burgers and advection–diffusion equations by using a semi-analytical iterative method," *Computers and Mathematics with Applications*, vol. 76, no. 1, pp. 155–171, 2018.

[10] J. Lou, L. Li, H. Luo, and H. Nishikawa, "Reconstructed discontinuous Galerkin methods for linear advection–diffusion equations based on first-order hyperbolic system," *Journal of Computational Physics*, vol. 369, pp. 103–124, 2018.

[11] H. Bhatt, A. Khaliq, and B. Wade, "Efficient Krylov-based exponential time differencing method in application to 3D advection-diffusion-reaction systems," *Applied Mathematics and Computation*, vol. 338, pp. 260–273, 2018.

[12] H. Cheng and G. Zheng, "Analyzing 3D advection-diffusion problems by using the improved element-free Galerkin method," *Mathematical Problems in Engineering*, vol. 2020, pp. 1–13, 2020.

[13] E. Cruz-Quintero and F. Jurado, "Boundary control for a certain class of reaction-advection-diffusion system," *Mathematics*, vol. 8, no. 11, pp. 1–22, 2020.

[14] K. Para, B. Jitsom, R. Eymard, S. Sungnul, S. Sirisubtawee, and S. Phongthanapanich, "An accuracy comparison of piecewise linear reconstruction techniques for the characteristic finite volume method for two-dimensional convection-diffusion equation," *ZAMM-Journal of Applied Mathematics and Mechanics/Zeitschrift für Angewandte Mathematik und Mechanik*, vol. 101, no. 2, pp. 1–21, 2021.

[15] H. Sun, Y. Xu, J. Lin, and Y. Zhang, "A space-time backward substitution method for three-dimensional advection-diffusion equations," *Computers and Mathematics with Applications*, vol. 97, pp. 77–85, 2021.

[16] M. I. P. Hidayat, "Meshless finite difference method with B-splines for numerical solution of coupled advection-diffusion-reaction problems," *International Journal of Thermal Sciences*, vol. 165, pp. 1–18, 2021.

[17] N. Shahid, M. A.-u. Rehman, A. Khalid, U. Fatima, T. S. Shaikh, N. Ahmed, H. Alotaibi, M. Rafiq, I. Khan, and K. S. Nisar, "Mathematical analysis and numerical investigation of advection-reaction-diffusion computer virus model," *Results in Physics*, vol. 26, pp. 1–10, 2021.

[18] O. F. Murillo-García and F. Jurado, "Adaptive boundary control for a certain class of reaction–advection–diffusion system," *Mathematics*, vol. 9, no. 18, pp. 1–17, 2021.

[19] I. Podlubny, *Fractional Differential Equations*. San Diego: Academic Press, 1999.

[20] M. Caputo, "Linear model of dissipation whose Q is almost frequency independent. II," *Geophysical Journal International*, vol. 13, no. 5, pp. 529–539, 1967.

[21] M. Caputo and M. Fabrizio, "A new definition of fractional derivative without singular kernel," *Progress in Fractional Differentiation and Applications*, vol. 1, pp. 73–85, 2015.

[22] A. Kilbas, "Hadamard-type fractional calculus," *Journal of The Korean Mathematical Society*, vol. 38, no. 6, pp. 1191–1204, 2001.

[23] R. Hilfer, *Applications of fractional calculus in physics*. Singapore: World Scientific, 2000.

[24] I. Ahmed, P. Kumam, F. Jarad, P. Borisut, and W. Jirakitpuwapat, "On hilfer generalized proportional fractional derivative," *Advances in Difference Equations*, vol. 2020, no. 1, pp. 1–18, 2020.

[25] U. N. Katugampola, "A new approach to generalized fractional derivatives," *Bulletin of Mathematical Analysis and Applications*, vol. 6, no. 4, pp. 1–15, 2014.

[26] A. Atangana and B. S. T. Alkahtani, "Extension of the resistance, inductance, capacitance electrical circuit to fractional derivative without singular kernel," *Advances in Mechanical Engineering*, vol. 7, no. 6, pp. 1–6, 2015.

[27] K. Hattaf, "On the stability and numerical scheme of fractional differential equations with application to biology," *Computation*, vol. 10, pp. 1–12, 2022.

[28] H. Khalid, "A new class of generalized fractal and fractal-fractional derivatives with non-singular kernels," *Fractal and Fractional*, vol. 7, no. 5, pp. 1–16, 2023.

[29] T. Langlands and B. I. Henry, "The accuracy and stability of an implicit solution method for the fractional diffusion equation," *Journal of Computational Physics*, vol. 205, no. 2, pp. 719–736, 2005.

[30] L. Su, W. Wang, and Z. Yang, "Finite difference approximations for the fractional advection–diffusion equation," *Physics Letters A*, vol. 373, no. 48, pp. 4405–4408, 2009.

[31] K. Wang and H. Wang, "A fast characteristic finite difference method for fractional advection–diffusion equations," *Advances in Water Resources*, vol. 34, no. 7, pp. 810–816, 2011.

[32] G. Zhong, M. Yi, and J. Huang, "Numerical method for solving fractional convection diffusion equations with time-space variable coefficients," *IAENG International Journal of Applied Mathematics*, vol. 48, no. 1, pp. 62–66, 2018.

[33] J. E. Macías-Díaz, "A dynamically consistent method to solve nonlinear multidimensional advection–reaction equations with fractional diffusion," *Journal of Computational Physics*, vol. 366, pp. 71–88, 2018.

[34] A. Jannelli, M. Ruggieri, and M. P. Speciale, "Analytical and numerical solutions of time and space fractional advection–diffusion–reaction equation," *Communications in Nonlinear Science and Numerical Simulation*, vol. 70, pp. 89–101, 2018.

[35] D. Vivek, E. Elsayed, and K. Kanagarajan, "Theory and analysis of partial differential equations with a ψ-Caputo fractional derivative," *Rocky Mountain Journal of Mathematics*, vol. 49, no. 4, pp. 1355–1370, 2019.

[36] A. El-Kahlout, "Exact solutions of partial differential equations of Caputo fractional order," *International Journal of Contemporary Mathematical Sciences*, vol. 16, no. 3, pp. 115–126, 2021.

[37] A. Qazza, R. Saadeh, and E. Salah, "Solving fractional partial differential equations via a new scheme," *AIMS Mathematics*, vol. 8, no. 3, pp. 5318–5337, 2023.

[38] Y. Dimitrov, S. Georgiev, and V. Todorov, "Approximation of caputo fractional derivative and numerical solutions of fractional differential equations," *Fractal and Fractional*, vol. 7, no. 10, pp. 1–26, 2023.

[39] N. Kumawat, A. Shukla, M. N. Mishra, R. Sharma, and R. S. Dubey, "Khalouta transform and applications to Caputo-fractional differential equations," *Frontiers of Applied Mathematics and Statistics*, vol. 10, pp. 1–10, 2024.

[40] P. Oyjinda and N. Pochai, "Numerical simulation to air pollution emission control near an industrial zone," *Advances in Mathematical Physics*, vol. 2017, pp. 1–7, 2017.

[41] K. Suebyat and N. Pochai, "Numerical simulation for a three-dimensional air pollution measurement model in a heavy traffic area under the Bangkok sky train platform," vol. 2018, pp. 1–10, 2018.

[42] J. Kusuma, A. Ribal, and A. G. Mahie, "On FTCS approach for Box model of three-dimension advection-diffusion equation," *International Journal of Differential Equations*, vol. 2018, no. 1, pp. 1–9, 2018.

[43] K. Pananu, S. Sungnul, S. Sirisubtawee, and S. Phongthanapanich, "Convergence and applications of the implicit finite difference method for advection-diffusion-reaction equations," *IAENG International Journal of Computer Science*, vol. 47, no. 4, pp. 645–663, 2020.

[44] K. Para, S. Sungnul, S. Sirisubtawee, and S. Phongthanapanich, "A comparison of numerical solutions for advection-diffusion-reaction equations between finite volume and finite difference methods," *Engineering Letters*, vol. 30, no. 2, pp. 566–581, 2022.

[45] P. D. Lax and R. D. Richtmyer, "Survey of the stability of linear finite difference equations," *Communications in Pure and Applied Mathematics*, vol. 9, no. 2, pp. 267–293, 1956.

[46] G. D. Smith, *Numerical Solution of Partial Differential Equations: Finite Difference Methods*, 3rd ed. Oxford University Press, 1985, iSBN 0-19-859641-3.

[47] J. C. Tannehill, D. Anderson, and R. H. Pletcher, *Computational Fluid Mechanics and Heat Transfer*, 2nd ed. Taylor and Francis, 1997.

[48] P. Zhuang and F. Liu, "Finite difference approximation for two-dimensional time fractional diffusion equation," *Journal of Algorithms & Computational Technology*, vol. 1, no. 1, pp. 1–16, 2007.

[49] M. Thongmoon, R. McKibbin, and S. Tangmanee, "Numerical solution of a 3-D advection-dispersion model for pollutant transport," *Thai Journal of Mathematics*, vol. 5, no. 1, pp. 91–108, 2012.

[50] K. Suebyat and N. Pochai, "A numerical simulation of a three-dimensional air quality model in an area under a Bangkok sky train platform using an explicit finite difference scheme," *IAENG International Journal of Applied Mathematics*, vol. 47, no. 4, pp. 471–476, 2017.

[51] R. Fazio, A. Jannelli, and S. Agreste, "A finite difference method on non-uniform meshes for time-fractional advection–diffusion equations with a source term," *Applied Sciences*, vol. 8, no. 6, pp. 1–16, 2018.